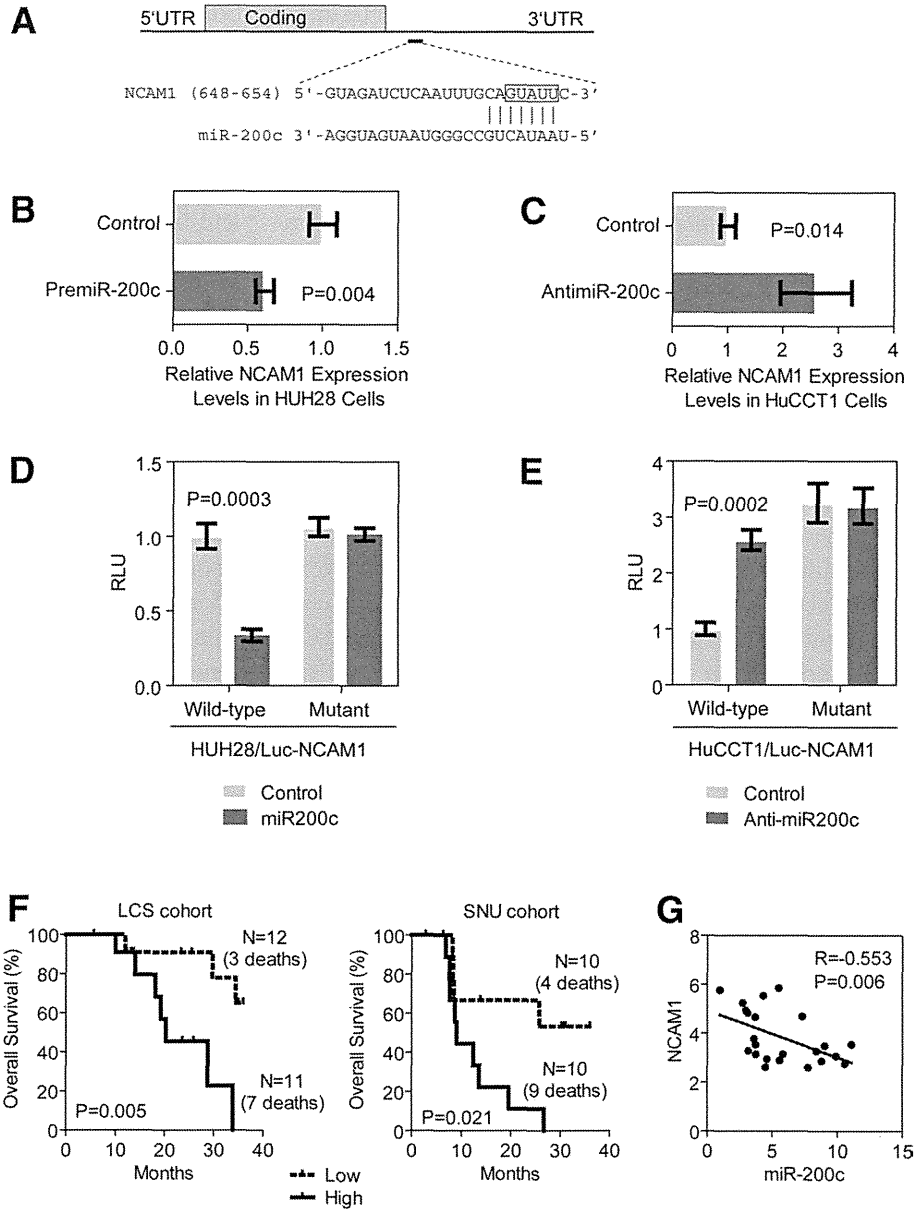

Fig. 7. Functional interactions between miR-200c and NCAM1. (A) Predicted duplex formation between the 3′UTR sequences of human NCAM1 and miR-200c where vertical bars represent the paired seed sequences. The box highlights the nucleotides that were changed to CAUAA in a mutant luciferase reporter. (B) Effect of premiR-200c oligo on NCAM1 expression in HuH28 cells as determined by qRT-PCR. (C) Effect of anti-miR-200c oligo on NCAM1 expression in HuCCT1 cells as determined by qRT-PCR. (D) Luciferase activities of wild-type and mutant reporters in HuH28 cells with or without the presence of pre-miR-200c oligo. (E) Luciferase activities of wildtype and mutant reporters in HuCCT1 cells with or without the presence of anti-miR200c oligo. Each experiment was repeated at least three times and the expression value is shown as the mean ± standard deviation. (F) Kaplan-Meier estimates of overall survival according to expression of NCAM1 in ICC cases from LCS and SNU cohorts. NCAM1 expression values were dichotomized into low and high groups using the within cohort median expression value as a cutoff. (G) Spearman correlation analysis of NCAM1 and miR-200c expression data as determined by mRNA and microRNA arrays.

ZEB2.[36,37] miR-200 family members are functionally linked to EMT, in part by way of targeting ZEB1 and ZEB2, as well as cell migration, invasion, and tumorigenicity.[36,38] These results suggest that the ZEB1-miR-200 feedback loop is critical for maintaining aggressive tumor features. In addition, we also found that miR-200c directly targets NCAM1. NCAM1 is highly expressed in hepatic stem cells and its function has been tightly linked to EMT.[29,39] Our results are consistent with the hypothesis that the miR-200-EMT gene axis may be functional critical to the development of stem-like ICC. Shared molecular activities including EMT and microRNA among HCC and ICC have been noted in recent publications.[40,41] Interestingly, abnormal regulation of EMT-related genes has been reported to be linked to HCC development.[42-44] However, no evidence has linked miR-200 to HCC development. Consistently, we found no evidence that miR-200c is silenced in stem-like HCC (data not shown). It is plausible that the miR-200c-EMT gene axis is a unique signaling pathway functionally important for stem-like ICC and could be exploited as molecular targets for ICC therapies. In addition, unlike HCC, EpCAM is not a good prognostic biomarker for ICC because its expression is highly elevated in both HpSC-ICC and MH-ICC (data not shown). Further studies involving in-depth analyses of miR-200c and EMT signaling and using relevant animal models would be needed to test the therapeutic relevance of these targets for ICC.

Human adult livers are believed to be comprised of maturational lineages of cells beginning intrahepatically

near the portal triads referred to as canals of Hering.[45] This region is close to intrahepatic bile ducts and is believed to contain liver stem cells. It is suggested that liver stem cells may give rise to bipotent progenitor cells, which have the potential to differentiate into both hepatocytic and cholangiocytic lineages. In principle, hepatic stem/progenitor cells could be the common cellular origin for both HCC and ICC. It is hypothesized that cancer progression is driven by the presence of CSC, which is also responsible for treatment resistance and tumor relapse.[46] CSCs have been demonstrated in a growing range of epithelial and other solid organ malignancies, suggesting that the majority of malignancies are dependent on such a compartment.[47] This model is attractive because it may help to address the heterogeneity of HCC and ICC, and could facilitate research strategies to define novel and effective therapies.[48] Consistently, studies on clinicopathological features of ICC suggest that some ICCs could arise from liver stem cells rather than from mature cholangiocytes.[49,50] Moreover, gene expression profiling revealed that some HCC cases contain ICC-like gene expression trait and embryonic stem cell-like traits.[15] These results suggest that certain types of ICC could be derived from the same cell origin that leads to HCC, whereas distinct mechanisms may be involved in the genesis of ICC.

CHC has been traditionally classified into three subtypes based on the histological description by Allen and Lisa in 1949.[51] These subtypes include type-A (collision or double cancer, which is referred to as separate HCC and ICC arising in the same liver), type-B (contiguous mass, which is referred to as admixed HCC/ICC such as fibrolamellar tumors), and type-C (transitional tumors, which are referred to as a tumor mass with cellular features of both HCC and ICC). In type-A tumors, the HCC and ICC lesions could be interpreted as originating separately from hepatocyte and bile duct epithelium. Type-B tumors could follow the same mechanism as type-A because it is difficult to distinguish them based on histological data. Because both HCC and ICC cellular features are intimately associated with the type-C tumors, they have been interpreted as arising from the same site and sharing the same cell origin. In our study, two Chinese and five Japanese CHC cases belong to type-B and seven Korean CHC cases[15] belong to type-C. Hierarchical clustering analyses revealed that both type-B and type-C CHC samples could be divided into stem-like ICC and mature hepatocyte-like ICC, which are also associated with survival (Fig. S8). Although these results are not conclusive due to limited cases, they appear consistent with the hypothesis that both type-B and type-C CHC could originate from the same hepatic progenitor cells shared by HCC and CHC tumors. A new histological subtyping of CHC according to the WHO Classification based on the presence of stem-cell features has been proposed.[52] Long-term follow-up of larger cohorts is needed to define the clinical and biological behavior of all CHC cases.

Our analysis dissecting the heterogeneous ICC based on the expression of stem cell-like signatures could classify ICC cases into subgroups with more uniform and prognostic phenotypes. In principle, targeting molecular pathways specific to each subpopulation would be more effective for the development of personalized clinical strategies. We suggest that the miR-200c-associated EMT pathway and stem-cell activities may contribute to the development of the HpSC-ICC tumors. The association of EMT with poor prognosis is well known in many cancer types. Moreover, recent studies have demonstrated the critical role of miR200c in the control of stem/progenitor cell renewal and differentiation. Our findings are consistent with the hypothesis supporting the pivotal role of miR-200c in the aggressive progression of stem-like ICC.

Acknowledgment: We thank Drs. Gregory J. Gores for H69 cells, Kathleen C. Flanders and Lalage M. Wakefield for anti-TGF-beta1 antibody, and Li Wang for the miR-200c luciferase reporter. We also thank Dr. Xiaolin Wu and members of the microarray core at the NCI-SAIC for help on microarray analysis and Ms. Karen Yarrick for bibliographic assistance.

References

1. Jemal A, Bray F, Center MM, Ferlay J, Ward E, Forman D.Global cancer statistics. CA Cancer J Clin 2011;61:69-90.
2. Martin R, Jarnagin W.Intrahepatic cholangiocarcinoma. Current management. Minerva Chir 2003;58:469-478.
3. Shaib Y, El-Serag HB.The epidemiology of cholangiocarcinoma. Semin Liver Dis 2004;24:115-125.
4. Berthiaume EP, Wands J.The molecular pathogenesis of cholangiocarcinoma. Semin Liver Dis 2004;24:127-137.
5. Komuta M, Spee B, Vander BS, De VR, Verslype C, Aerts R, et al. Clinicopathological study on cholangiolocellular carcinoma suggesting hepatic progenitor cell origin. HEPATOLOGY 2008;47:1544-1556.
6. Zhou H, Wang H, Zhou D, Wang H, Wang Q, Zou S, et al. Hepatitis B virus-associated intrahepatic cholangiocarcinoma and hepatocellular carcinoma may hold common disease process for carcinogenesis. Eur J Cancer 2010;46:1056-1061.
7. Lee JS, Heo J, Libbrecht L, Chu IS, Kaposi-Novak P, Calvisi DF, et al. A novel prognostic subtype of human hepatocellular carcinoma derived from hepatic progenitor cells. Nat Med 2006;12:410-416.
8. Yamashita T, Ji J, Budhu A, Forgues M, Yang W, Wang HY, et al. EpCAM-positive hepatocellular carcinoma cells are tumor-initiating cells with stem/progenitor cell features. Gastroenterology 2009;136:1012-1024.
9. Yamashita T, Forgues M, Wang W, Kim JW, Ye Q, Jia H, et al. EpCAM and alpha-fetoprotein expression defines novel prognostic subtypes of hepatocellular carcinoma. Cancer Res 2008;68:1451-1461.

10. Cairo S, Wang Y, de RA, Duroure K, Dahan J, Redon MJ, et al. Stem cell-like micro-RNA signature driven by Myc in aggressive liver cancer. Proc Natl Acad Sci U S A 2010;107:20471-20476.
11. Ma S, Chan KW, Hu L, Lee TK, Wo JY, Ng IO, et al. Identification and characterization of tumorigenic liver cancer stem/progenitor cells. Gastroenterology 2007;132:2542-2556.
12. Yang ZF, Ho DW, Ng MN, Lau CK, Yu WC, Ngai P, et al. Significance of CD90(+) cancer stem cells in human liver cancer. Cancer Cell 2008;13:153-166.
13. Haraguchi N, Ishii H, Mimori K, Tanaka F, Ohkuma M, Kim HM, et al. CD13 is a therapeutic target in human liver cancer stem cells. J Clin Invest 2010;120:3326-3339.
14. Tang Y, Kitisin K, Jogunoori W, Li C, Deng CX, Mueller SC, et al. Progenitor/stem cells give rise to liver cancer due to aberrant TGF-beta and IL-6 signaling. Proc Natl Acad Sci U S A 2008;105:2445-2450.
15. Woo HG, Lee JH, Yoon JH, Kim CY, Lee HS, Jang JJ, et al. Identification of a cholangiocarcinoma-like gene expression trait in hepatocellular carcinoma. Cancer Res 2010;70:3034-3041.
16. Budhu A, Forgues M, Ye QH, Jia LH, He P, Zanetti KA, et al. Prediction of venous metastases, recurrence and prognosis in hepatocellular carcinoma based on a unique immune response signature of the liver microenvironment. Cancer Cell 2006;10:99-111.
17. Budhu A, Jia HL, Forgues M, Liu CG, Goldstein D, Lam A, et al. Identification of metastasis-related microRNAs in hepatocellular carcinoma. HEPATOLOGY 2008;47:897-907.
18. Ji J, Yamashita T, Budhu A, Forgues M, Jia HL, Li C, et al. Identification of microRNA-181 by genome-wide screening as a critical player in EpCAM-positive hepatic cancer stem cells. HEPATOLOGY 2009;50:472-480.
19. Ji J, Shi J, Budhu A, Yu Z, Forgues M, Roessler S, et al. MicroRNA expression, survival, and response to interferon in liver cancer. N Engl J Med 2009;361:1437-1447.
20. Ye QH, Qin LX, Forgues M, He P, Kim JW, Peng AC, et al. Predicting hepatitis B virus-positive metastatic hepatocellular carcinomas using gene expression profiling and supervised machine learning. Nat Med 2003;9:416-423.
21. Woo HG, Wang XW, Budhu A, Kim YH, Kwon SM, Tang ZY, et al. Association of TP53 mutations with stem cell-like gene expression and survival of patients with hepatocellular carcinoma. Gastroenterology 2011;140:1063-1070.e8.
22. Woo HG, Park ES, Lee JS, Lee YH, Ishikawa T, Kim YJ, et al. Identification of potential driver genes in human liver carcinoma by genome-wide screening. Cancer Res 2009;69:4059-4066.
23. Andersen JB, Spee B, Blechacz BR, Avital I, Komuta M, Barbour A, et al. Genomic and genetic characterization of cholangiocarcinoma identifies therapeutic targets for tyrosine kinase inhibitors. Gastroenterology 2012;142:1021-1031.
24. Park J, Gores GJ, Patel T. Lipopolysaccharide induces cholangiocyte proliferation via an interleukin-6-mediated activation of p44/p42 mitogen-activated protein kinase. HEPATOLOGY 1999;29:1037-1043.
25. Zhang Y, Yang Z, Whitby R, Wang L.Regulation of miR-200c by nuclear receptors PPARalpha, LRH-1 and SHP. Biochem Biophys Res Commun 2011;416:135-139.
26. Roessler S, Jia HL, Budhu A, Forgues M, Ye QH, Lee JS, et al. A unique metastasis gene signature enables prediction of tumor relapse in early-stage hepatocellular carcinoma patients. Cancer Res 2010;70:10202-10212.
27. Meng F, Henson R, Lang M, Wehbe H, Maheshwari S, Mendell JT, et al. Involvement of human micro-RNA in growth and response to chemotherapy in human cholangiocarcinoma cell lines. Gastroenterology 2006;130:2113-2129.
28. Mott JL, Kobayashi S, Bronk SF, Gores GJ.mir-29 regulates Mcl-1 protein expression and apoptosis. Oncogene 2007;26:6133-6140.
29. Turner R, Lozoya O, Wang Y, Cardinale V, Gaudio E, Alpini G, et al. Human hepatic stem cell and maturational liver lineage biology. HEPATOLOGY 2011;53:1035-1045.
30. Kalluri R, Weinberg RA.The basics of epithelial-mesenchymal transition. J Clin Invest 2009;119:1420-1428.
31. Yang J, Mani SA, Donaher JL, Ramaswamy S, Itzykson RA, Come C, et al. Twist, a master regulator of morphogenesis, plays an essential role in tumor metastasis. Cell 2004;117:927-939.
32. Oft M, Heider KH, Beug H.TGFbeta signaling is necessary for carcinoma cell invasiveness and metastasis. Curr Biol 1998;8:1243-1252.
33. Heldin CH, Landstrom M, Moustakas A.Mechanism of TGF-beta signaling to growth arrest, apoptosis, and epithelial-mesenchymal transition. Curr Opin Cell Biol 2009;21:166-176.
34. Nawshad A, Lagamba D, Polad A, Hay ED.Transforming growth factor-beta signaling during epithelial-mesenchymal transformation: implications for embryogenesis and tumor metastasis. Cells Tissues Organs 2005;179:11-23.
35. Pardali K, Moustakas A.Actions of TGF-beta as tumor suppressor and pro-metastatic factor in human cancer. Biochim Biophys Acta 2007;1775:21-62.
36. Burk U, Schubert J, Wellner U, Schmalhofer O, Vincan E, Spaderna S, et al. A reciprocal repression between ZEB1 and members of the miR-200 family promotes EMT and invasion in cancer cells. EMBO Rep 2008;9:582-589.
37. Park SM, Gaur AB, Lengyel E, Peter ME.The miR-200 family determines the epithelial phenotype of cancer cells by targeting the E-cadherin repressors ZEB1 and ZEB2. Genes Dev 2008;22:894-907.
38. Wellner U, Schubert J, Burk UC, Schmalhofer O, Zhu F, Sonntag A, et al. The EMT-activator ZEB1 promotes tumorigenicity by repressing stemness-inhibiting microRNAs. Nat Cell Biol 2009;11:1487-1495.
39. Frame MC, Inman GJ.NCAM is at the heart of reciprocal regulation of E-cadherin- and integrin-mediated adhesions via signaling modulation. Dev Cell 2008;15:494-496.
40. Seok JY, Na DC, Woo HG, Roncalli M, Kwon SM, Yoo JE, et al. A fibrous stromal component in hepatocellular carcinoma reveals a cholangiocarcinoma-like gene expression trait and EMT. HEPATOLOGY 2012;55:1776-1786.
41. Meng F, Glaser SS, Francis H, DeMorrow S, Han Y, Passarini JD, et al. Functional analysis of microRNAs in human hepatocellular cancer stem cells. J Cell Mol Med 2012;16:160-173.
42. Giannelli G, Bergamini C, Fransvea E, Sgarra C, Antonaci S.Laminin-5 with transforming growth factor-beta1 induces epithelial to mesenchymal transition in hepatocellular carcinoma. Gastroenterology 2005;129:1375-1383.
43. Lee TK, Poon RT, Yuen AP, Ling MT, Kwok WK, Wang XH, et al. Twist overexpression correlates with hepatocellular carcinoma metastasis through induction of epithelial-mesenchymal transition. Clin Cancer Res 2006;12:5369-5376.
44. Jou J, Diehl AM.Epithelial-mesenchymal transitions and hepatocarcinogenesis. J Clin Invest 2010;120:1031-1034.
45. Sigal SH, Brill S, Fiorino AS, Reid LM. The liver as a stem cell and lineage system. Am J Physiol 1992;263:G139-G148.
46. Clevers H.The cancer stem cell: premises, promises and challenges. Nat Med 2011;17:313-319.
47. Alison MR, Islam S, Wright NA. Stem cells in cancer: instigators and propagators? J Cell Sci 2010;123:2357-2368.
48. Oishi N, Wang XW.Novel therapeutic strategies for targeting liver cancer stem cells. Int J Biol Sci 2011;7:517-535.
49. Lee JH, Rim HJ, Sell S.Heterogeneity of the "oval-cell" response in the hamster liver during cholangiocarcinogenesis following Clonorchis sinensis infection and dimethylnitrosamine treatment. J Hepatol 1997;26:1313-1323.
50. Ishii T, Yasuchika K, Suemori H, Nakatsuji N, Ikai I, Uemoto S.Alpha-fetoprotein producing cells act as cancer progenitor cells in human cholangiocarcinoma. Cancer Lett 2010;294:25-34.
51. Allen RA, Lisa JR.Combined liver cell and bile duct carcinoma. Am J Pathol 1949;25:647-655.
52. Theise ND, Nakashima O, Park YN, Nakanuma Y. Combined hepatocellular-cholangiocarcinoma. In: Bosman FT, Carneiro F, Hruban RH, Theise ND, editors. WHO classification of tumours of the digestive system. Lyon, France: World Health Organization; 2010:225-227.

STEM CELLS AND DEVELOPMENT
Volume 21, Number 16, 2012

DOI: 10.1089/scd.2011.0725

Nucleostemin in Injury-Induced Liver Regeneration

Haruhiko Shugo,[1,2,*] Takako Ooshio,[1,*] Masako Naito,[1] Kazuhito Naka,[1] Takayuki Hoshii,[1] Yuko Tadokoro,[1] Teruyuki Muraguchi,[1] Akira Tamase,[1] Noriyuki Uema,[1] Taro Yamashita,[2] Yasunari Nakamoto,[2] Toshio Suda,[3] Shuichi Kaneko,[2] and Atsushi Hirao[1]

The high regenerative capacity of liver contributes to the maintenance of its size and function when injury occurs. Partial hepatectomy induces division of mature hepatocytes to maintain liver function, whereas severe injury stimulates expansion of undifferentiated hepatic precursor cells, which supply mature cells. Although several factors reportedly function in liver regeneration, the precise mechanisms underlying regeneration remain unclear. In this study, we analyzed expression of nucleostemin (NS) during development and in injured liver by using transgenic green fluorescent protein reporter (NS-GFP Tg) mice. In neonatal liver, the hepatic precursor cells that give rise to mature hepatocytes were enriched in a cell population expressing high levels of NS. In adult liver, NS was abundantly expressed in mature hepatocytes and rapidly upregulated by partial hepatectomy. Severe liver injury promoted by a diet containing 3,5-diethoxycarbonyl-1,4-dihydrocollidine induced the emergence of NS-expressing ductal epithelial cells as hepatic precursor cells. NS knockdown inhibited both hepatic colony formation in vitro and proliferation of hepatocytes in vivo. These data strongly suggest that NS plays a critical role in regeneration of both hepatic precursor cells and hepatocytes in response to liver injury.

Introduction

THE LIVER IS AN ORGAN WITH high regenerative capacity, enabling it to maintain a constant size and function following injury [1,2]. In resting liver, hepatocytes are quiescent and rarely undergo cell division. Therefore, hepatocyte replacement occurs slowly in static conditions. However, when the liver is injured, cells replicate to restore loss of tissue mass and function. Proliferation of hepatocytes and bile duct epithelial cells contributes to liver maintenance. After partial hepatectomy, the remaining lobes regenerate the entire liver mass within 5–7 days, a process accomplished primarily by division of mature cells rather than of stem/precursor cells. In mice, division of hepatocytes starts after partial hepatectomy and is maximal 24–48 h later. Several molecules, including hepatocyte growth factor (HGF), interleukin-6, tumor necrosis factor α, transforming growth factor, and epidermal growth factor (EGF), reportedly govern this process [1,2]. Termination of regeneration is also important for the maintenance of homeostasis. In severe injury associated with defects in hepatocyte proliferation, it is believed that bipotential precursors of hepatocytes and cholangiocytes contribute to liver regeneration [3,4]. Currently, it is thought that potential hepatic precursor cells emerge from smaller branches of the biliary tree. In rats, a population of small cells exhibiting large nuclei, called oval cells, emerges around portal veins following liver injury [5]. In mice, a diet supplemented with 3,5-diethoxycarbonyl-1,4-dihydrocollidine (DDC) induces ductal proliferation and morphological changes similar to those seen in the rat oval cell response [6]. Precursor cells appear to regenerate hepatocytes and cholangiocytes through proliferation, migration, and differentiation processes. Thus, proper control of both mature cells and hepatic stem/precursor cells is critical for liver regeneration.

Nucleostemin (NS) is a GTPase that binds to p53 and was originally reported to be highly expressed in stem cells from several tissues, including embryonic stem (ES) cells, immature hematopoietic cells, and neural stem/progenitor cells [7]. NS loss results in reduced cell proliferation and increased apoptosis in both ES cells and ES cell-derived neural stem/progenitor cells [8]. Structural comparisons have been used to isolate NS homologues in *Caenorhabditis elegans* [9], newt [10], *Xenopus* [11], mouse [7], and human [12]. In the regenerating newt lens, NS protein rapidly accumulates in nucleoli of dedifferentiating pigmented epithelial cells and multinucleate muscle fibers [10], suggesting that its expression correlates with undifferentiated status in newt cells. In contrast, the NS homologue in *Caenorhabditis elegans* (*nst-1*) is expressed in both proliferating and differentiated cells. *Nst-1* mutants exhibit defects in larval growth and cell cycle

[1]Division of Molecular Genetics, Cancer Research Institute, Kanazawa University, Kanazawa, Japan.
[2]Disease Control and Homeostasis, Kanazawa University Graduate School of Medical Science, Kanazawa, Japan.
[3]Department of Cell Differentiation, The Sakaguchi Laboratory of Developmental Biology, Keio University School of Medicine, Tokyo, Japan.
*These authors contributed equally to this work.

progression in germline stem cells [9]. Because *nst-1*-mutant germ cells can still differentiate into mature sperm, nst-1 may play a critical role in germline stem cell proliferation but not in differentiation. In addition, NS is reportedly expressed at similar levels in non-proliferating muscle stem cells (satellite cells), rapidly proliferating precursor cells (myoblasts), and post-mitotic terminally differentiated cells (myotubes and myofibers) [13]. NS downregulation inhibits differentiation of myoblasts to myotubes, suggesting a role in post-mitotic terminal differentiation in this type. Thus, NS has pleiotropic effects on cellular function, and it is unclear how NS is involved in cell differentiation.

In a previous study, we generated a reporter system where the NS promoter drives green fluorescent protein (GFP) expression (termed NS-GFP) in vivo [14]. We successfully used this reporter system to identify a specific fraction of neonatal germ cells as spermatogonial stem cells with long-term repopulating capacity. We also combined the NS reporter system with a mouse brain tumor model and demonstrated the existence of an undifferentiated tumor-initiating cell (TIC) population in a highly aggressive brain tumor by analyzing GFP fluorescence intensity [15]. Consistent with our data, a recent report employing a bacterial artificial chromosome transgenic mouse line expressing GFP from the NS promoter showed that NS-enriched mammary tumor cells are highly tumorigenic in vitro and in vivo [16]. Further, another recent report showed that NS overexpression enhanced tumorigenicity of TICs, increased expression of genes that maintain undifferentiated status, and enhanced radioresistance [17]. These data suggest that NS functions to maintain stem cell properties in malignant cells.

In this study, we examined the expression and function of NS in liver. Interestingly, we found that NS contributes to the proliferation of hepatocytes after partial hepatectomy and to the regenerative capacity of hepatic precursor cells. Our data strongly suggest that NS is essential for injury-induced liver regeneration.

Materials and Methods

Animals

Mice used in this study were on a C57BL/6 background. NS-GFP Tg mice were generated as described previously [14]. Livers were collected at fetal (embryonic day 14.5: E14.5), neonatal (postnatal day 5: P5), and adult (8 weeks old) stages. For experiments involving severe liver injury, adult mice were fed a diet containing 0.1% DDC (Sigma-Aldrich, St. Louis, MO) for 2 weeks [6]. For partial hepatectomy, mice were anesthetized and 70% of the liver was resected. All procedures were performed in accordance with the animal care guidelines of Kanazawa University.

Isolation of liver cells

For digestion of fetal or neonatal liver cells, livers were minced and dissociated with enzyme-based dissociation buffer (Invitrogen Life Technologies, Carlsbad, CA) as described previously [18]. For isolation of adult liver cells, a 2-step perfusion method was utilized [19]. Briefly, perfusion collagenase solution (0.5 g/L; Sigma-Aldrich) was administered to a sacrificed mouse via the portal vein. Nonparenchymal cells were separated from parenchymal cells by centrifugation (50 *g*, 1 min), and dead cells were removed by centrifugation through 25% Percoll solution (GE Healthcare, Tokyo, Japan).

Flow cytometry

Single-cell suspensions from fetal, neonatal, or adult liver were incubated with an anti-CD16/CD32 antibody on ice for 10 min, followed by incubation with phycoerythrin (PE)-conjugated anti-TER119 and anti-CD45 antibodies (BD Pharmingen, San Diego, CA) on ice for 30 min. Cells were washed thrice in staining solution [2% fetal calf serum (FCS)/phosphate-buffered saline (PBS)] and incubated with anti-PE microbeads (Miltenyi Biotech, Bergisch Gladbach, Germany). After 3 washes, $CD45^{-}TER119^{-}$cells were collected (MACS; Miltenyi Biotech). Fetal liver cells were incubated with a biotin-conjugated anti-Dlk antibody (MBL, Nagoya, Japan), followed by incubation with allophycocyanin-conjugated streptavidin antibody (BD Pharmingen). Dead cells were stained with propidium iodide. Fluorescence-labeled cells were analyzed and sorted with JSAN (Bay Bioscience Co, Kobe, Japan).

Hepatic colony forming assay

Cells fractionated by flow cytometry were inoculated at 2,500 cells/well into six-well dishes coated with type I collagen (0.3 mg/mL; Nitta Gelatin, Osaka, Japan). The culture medium included Dulbecco's modified Eagle medium (DMEM)/F-12 supplemented with 10% fetal bovine serum, 5 mmol/L HEPES (Wako, Osaka, Japan), 200 μmol/L L-glutamine (Invitrogen Life Technologies), 50 μmol/L 2-mercaptoethanol (Sigma-Aldrich), 10 mmol/L nicotinamide (Sigma-Aldrich), 10^{-7} mol/L dexamethasone (Sigma-Aldrich), 1 mg/L insulin (Wako), 1× penicillin/streptomycin (Invitrogen Life Technologies), 50 ng/mL HGF (Peprotech, Rocky Hill, NJ), and 20 ng/mL EGF (Sigma-Aldrich).

Immunohistochemical analyses

Adult liver tissues were fixed with 4% paraformaldehyde at 4°C overnight and embedded in paraffin. Frozen sections were sliced and then fixed with 4% paraformaldehyde. The following primary antibodies were used: goat anti-NS (1:200; R&D Systems, Inc., Minneapolis, MN), rabbit anti-GFP (1:500; Invitrogen Life Technologies), and mouse anti-Ki-67 (1:200; BD Pharmingen). Sections were incubated with primary antibodies for 16 h at 4°C, followed by incubation with the appropriate Alexa Fluor dye conjugated to anti-goat IgG, anti-rabbit IgG, or anti-mouse IgG secondary antibodies (all 1:200; Molecular Probes, Inc., Eugene, OR). Staining was visualized using confocal microscopy (FV1000; Olympus, Tokyo, Japan). For some experiments, primary antibodies were detected using peroxidase-conjugated secondary antibodies (GE Healthcare, Amersham, Buckinghamshire, UK) in combination with a 3, 3'-diaminobenzidine (DAB) Peroxidase Substrate Kit (Vector Laboratories, Burlingame, CA). Sections were counterstained with Mayer's hematoxylin and analyzed using a microscope (Ax80; Olympus).

Immunocytochemical analyses

Hepatic colonies or cell lines were fixed with 4% paraformaldehyde for 10 min, followed by incubation with goat anti-albumin (1:100; Bethyl Laboratories, Montgomery, TX),

rabbit anti-cytokeratin 19 (1:1,000, a gift from Dr. Atsushi Miyajima), chicken anti-GFP (1:500; AVES, Tigard, OR), and/or mouse anti-Ki-67 (1:200; BD Pharmingen) at 4°C overnight and then stained with Alexa 546–conjugated and/or Alexa 488–conjugated secondary antibodies.

Western blotting analyses

Liver samples were lysed with sodium dodecyl sulfate (SDS)–polyacrylamide gel electrophoresis (PAGE) sample buffer, sonicated, boiled, and used as total liver cell lysates. Protein concentrations were measured by the bicinchoninic acid (BCA) protein assay (Pierce, Rockford, IL), and equal amounts of protein were separated by SDS-PAGE and transferred onto polyvinylidene difluoride (PVDF) membranes. Membranes were blocked with 5% skim milk in PBS containing Tween 20 for 1 h at room temperature. Membranes were then incubated with a goat anti-NS antibody (1:1,000; Neuromics, Edina, MN) for 16 h at 4°C and a mouse anti-β-actin antibody (1:1,000; Sigma-Aldrich) for 1 h at room temperature. Immune complexes were detected using peroxidase-conjugated secondary antibodies (1:1,000; GE Healthcare and DAKO, Glostrup, Denmark) for 30 min at room temperature and the ECL Prime western blotting detection system (GE Healthcare).

Reverse transcription–polymerase chain reaction

An RNeasy Mini Kit (Qiagen GmbH, Germany) was used in accordance with the manufacturer's instructions to extract total RNA from nonparenchymal cells sorted by fluorescence-activated cell sorting from adult mice treated with DDC. The primers used were as follows: GAPDH (5′-ACCA CAGTCCATGCCATCAC-3′ and 5′-TCCACCACCCTGTTG CTGTA-3′), NS (5′-TCGGAGTCCAGCAAGCATTG-3′ and 5′-GCAGCACTTTCCACATTTGGG-3′), CK19 (5′-GTCCTAC AGATTGACATTGC-3′ and 5′-CACGCTCTGGATCTGTGA CAG-3′), EpCAM (5′-AGGGGCGATCCAGAACAACG-3′ and 5′-ATGGTCGTAGGGGCTTTCTC-3′), Prominin1 (5′-GTA CCTCAGATCCAGCCAGCAA-3′ and 5′-ATTCTTCCAGCT

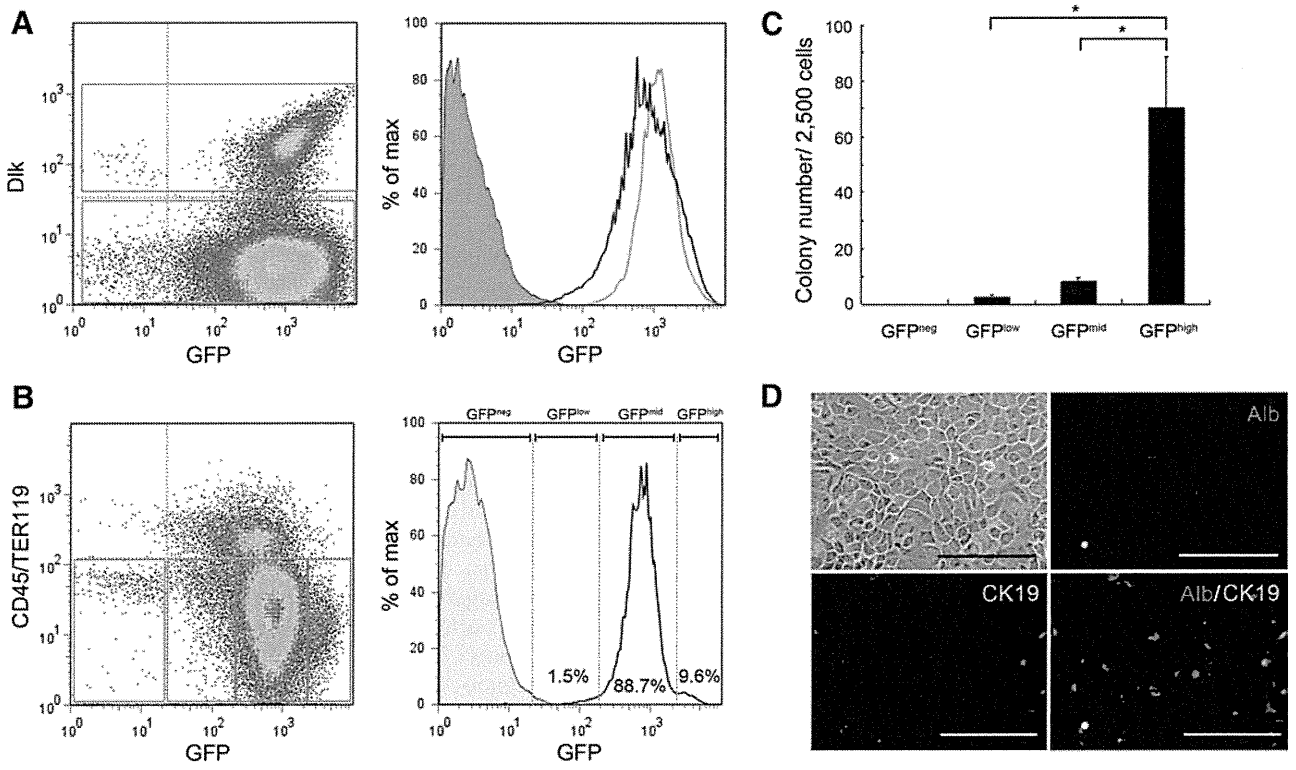

FIG. 1. Correlation of nucleostemin (NS) expression with colony-forming capacity of hepatic precursor cells in developing liver. **(A)** Flow cytometry analysis of green fluorescent protein (GFP) expression in NS-GFP Tg fetal liver. Nonhematopoietic cells from fetal liver cells at E14.5 were isolated by depletion of $CD45^+Ter119^+$ cells. *Left panel*: flow cytometry analysis of Dlk and GFP in $CD45^-Ter119^-$cells. *Right panel*: histogram of GFP expression. GFP expression in Dlk^+ cells (*gray line*) was slightly higher than that seen in Dlk^- cells (*black line*). *Gray region*: wild-type control mouse. The data shown are representative of 3 independent experiments. **(B)** Flow cytometry analysis of GFP expression in NS-GFP Tg neonatal liver. Flow cytometry analysis with CD45/Ter119 and GFP, and histogram with GFP in $CD45^-Ter119^-$ (nonhematopoietic cells) from neonatal liver (P5) are shown in the *left* and *right panels*, respectively. Nonhematopoietic cells ($CD45^-Ter119^-$) were fractionated into GFP^{neg}, GFP^{low}, GFP^{mid}, and GFP^{high} subpopulations. Values in panels are the percentage of the specified subpopulation among $CD45^-Ter119^-$ cells. The data shown are representative of 5 independent experiments. **(C)** Hepatic colony formation of subpopulations in **(B)**. Fractionated cells in **(B)** were cultured for 5 days. Data shown are the mean number ± standard deviation (SD) of colonies ($n = 3$). $^*P < 0.01$ **(D)** Characterization of hepatic colonies. Colonies (brightfield, *upper left panel*) were fixed and stained with anti-albumin (*red*) and anti-CK19 (*green*) antibodies. Most colonies in the culture express albumin or CK19. Representative data are shown. Scale bars, 100 μm.

TGGGCAGC-3'), and CD44 (5'-GGCTTTCAACAGTACC TTAC-3' and 5'-TGAAGCAATATGTGTCATAG-3').

Lentiviral transduction of short hairpin RNA

To downregulate NS in hepatic precursor cells or mouse hepatic cell lines (Hepa1-6, a mouse hepatocellular carcinoma cell line and BNL C1. 2, a mouse embryonic liver cell line), lentiviruses carrying short hairpin RNA (shRNA) against NS was prepared as previously described [14]. Oligonucleotides encoding shRNA directed against mouse NS mRNA were synthesized as follows: NS #1: sense, AGTAGA AATTTGATGGGCA; antisense, AGCAGAAACTTGATAG GCA; NS #2: sense, GAGGAAAGTTGTTTCGTTA; antisense, GAAGAAAGTTGTTCCATTA. Hepatic colonies derived from Dlk^+ fetal liver cells or cell lines were infected with lentivirus for 12 h, followed by washes with PBS, and incubation with culture medium. Cell lines were cultured with 10% FCS/DMEM (Invitrogen Life Technologies).

NS knockdown by hydrodynamic shRNA injection

In vivo transfection of shRNA plasmids into hepatocytes was performed by hydrodynamic injection using 6-week-old mice 3 days prior to partial hepatectomy, in accordance with a previous report [20]. A 27-gauge needle was used to inject 40 μg of plasmid in 2 mL PBS through the tail vein within 10 s. Three days later, the animals were sacrificed and the livers were fixed with 4% paraformaldehyde in PBS and embedded in paraffin for sectioning.

Statistical analyses

Statistical differences were determined using the unpaired Student's *t*-test for *P* values.

Results

NS expression correlates with the colony-forming capacity of hepatic precursor cells in developing liver

To investigate NS expression in developing liver, we evaluated GFP intensity in liver cells of NS-GFP Tg fetuses (E14.5) and neonates (P5). Flow cytometry analysis of fetal liver cells showed that most $CD45^-Ter119^-$ (non-hematopoietic) cells expressed high GFP levels (Fig. 1A). Although GFP levels were very high in Dlk^+ cells, in which hepatic stem/precursor cells are enriched [21], those levels were only slightly higher than those in Dlk^- cells (Fig. 1A). Thus, GFP expression was not indicative of a particular subpopulation in fetal liver. Interestingly, however, NS-GFP neonatal liver cells fell into distinct populations based on GFP

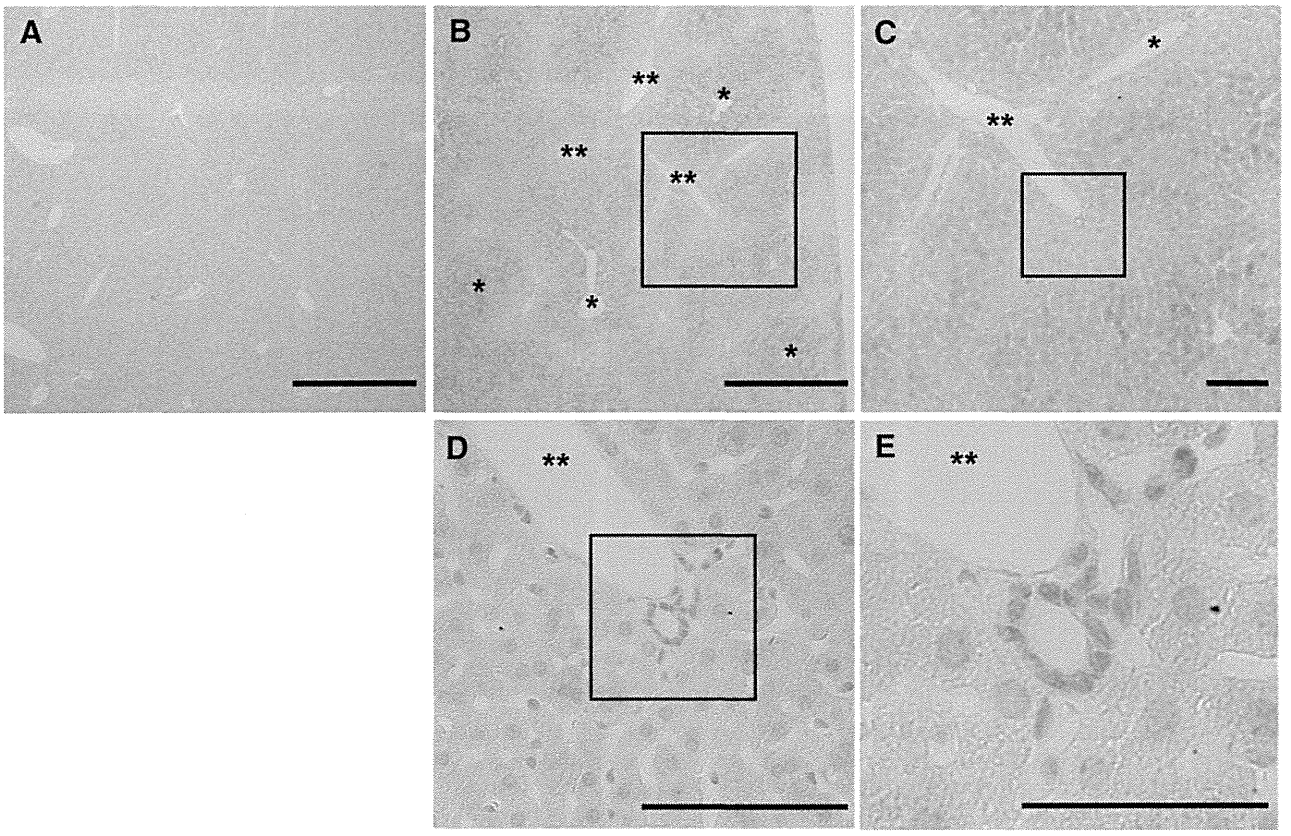

FIG. 2. Expression of NS-GFP in hepatocytes and bile duct epithelial cells of adult liver. **(A–E)** Immunohistochemical analyses of GFP in livers of adult mice (8 weeks old). Sections were stained with an anti-GFP antibody (*brown*), followed by a 3, 3'-diaminobenzidine (DAB) peroxidase reaction. **(A)** Wild-type control (C57BL/6) mice. **(B–E)** NS-GFP Tg mice. **(B)**, **(C)**, and **(D)** are lower-power views of areas shown at higher power in **(C)**, **(D)**, and **(E)**, respectively. Scale bars, 500 μm **(A, B)**, 100 μm **(C, D)**, 50 μm **(E)**, *central vein, **portal vein.

fluorescence intensity (Fig. 1B). While most non-hematopoietic cells were GFP^{mid}, we found a distinct GFP^{high} population. The proportions of GFP^{low} and GFP^{neg} cells were very small. To determine the potential functional significance of these subpopulations, we evaluated hepatic colony forming ability. GFP^{high} cells generated colonies at higher frequency than did any other cell population (Fig. 1C). Most colonies derived from GFP^{high} cells were $CK19^{+}$ or $albumin^{+}$ hepatocytes (Fig. 1D), suggesting that NS is an indicator of hepatic precursor cells in neonatal liver.

Partial hepatectomy upregulates NS expression in hepatocytes

We next examined NS-GFP expression in adult liver. We found that NS-GFP is highly expressed in hepatocytes. In

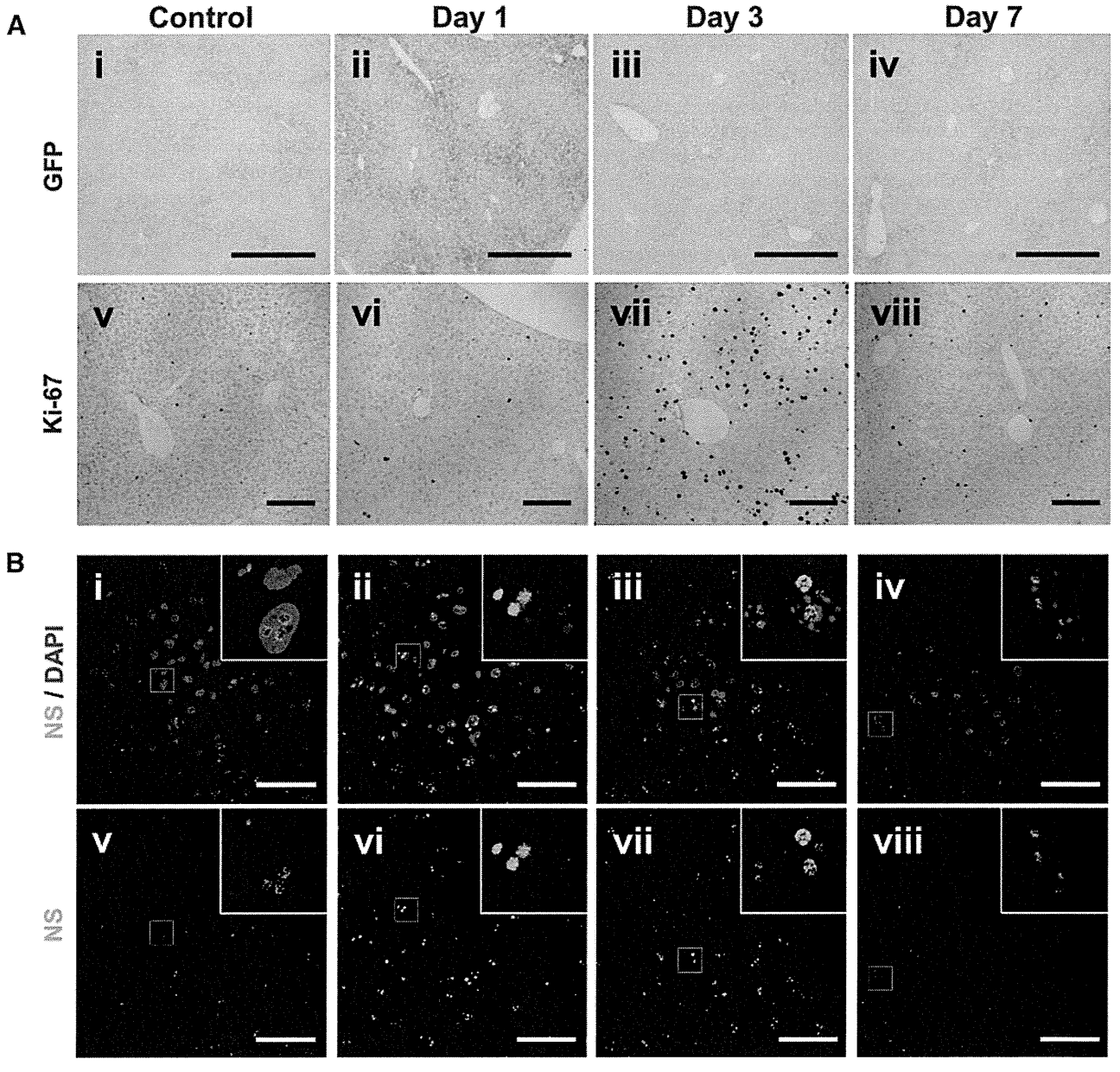

FIG. 3. Upregulation of NS-GFP in adult hepatocytes in response to partial hepatectomy. **(A)** Immunohistochemical analyses of GFP in liver of adult NS-GFP Tg mice after partial hepatectomy. Sections were stained with anti-GFP **(i–iv,** *brown***)** or anti-Ki-67 antibodies **(v–viii,** *brown***)**, followed by DAB peroxidase reactions. **(i, v)** control, **(ii, vi)** day 1, **(iii, vii)** day 3, **(iv, viii)** day 7. Scale bars, 500 μm **(i–iv)**, 100 μm **(v–viii)**. **(B)** Immunohistochemical analyses of endogenous NS in liver of adult NS-GFP Tg mice after partial hepatectomy. Liver sections were stained with an anti-NS antibody, followed by a secondary antibody conjugated to Alexa 488 **(***green***, i–viii)** plus DAPI **(**nuclear staining, *blue*, **i–iv)**. **(i, v)** control, **(ii, vi)** day 1, **(iii, vii)** day 3, **(iv, viii)** day 7. Scale bars, 50 μm. *Insets* are magnified views of the indicated areas. **(C)** Western blotting analyses of endogenous NS in liver of adult wild-type mice after partial hepatectomy. Lysates were prepared from liver (3 independent samples for each group) and immunoblotted to detect NS and β-actin as a loading control. Short and long exposures are shown for NS in the *upper* and *middle panels*, respectively.

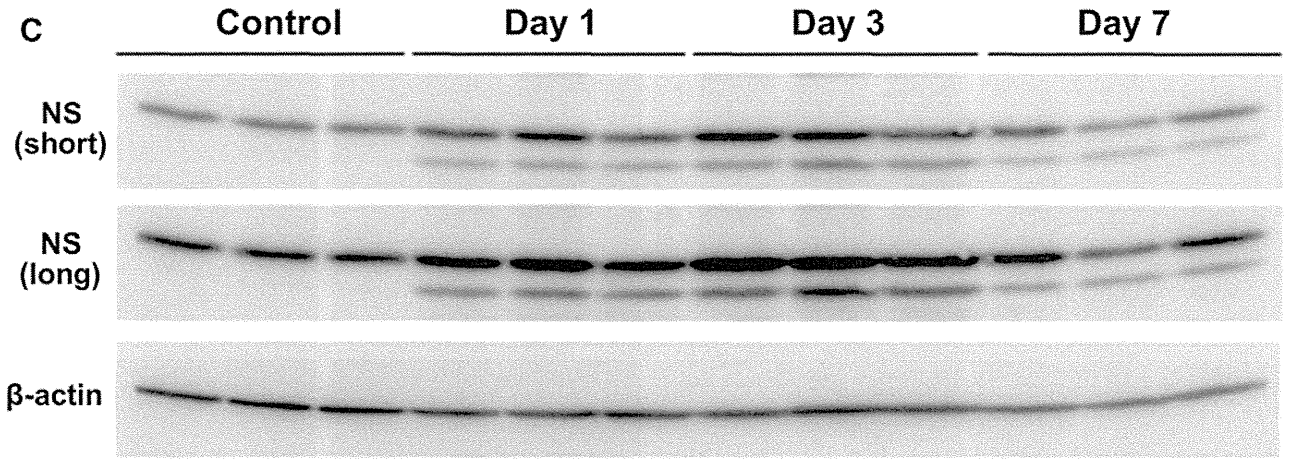

FIG. 3. (Continued).

particular, hepatocytes near central veins showed higher levels of NS-GFP expression than did those in the portal area (Fig. 2A–C). In addition, we found that NS-GFP is also highly expressed in bile duct epithelial cells (Fig. 2D, E). Next, we asked whether expression levels of NS-GFP are altered by liver injury. After partial hepatectomy, NS-GFP was upregulated within 24 h (Fig. 3A i–iv). Immunohistochemical analyses showed that NS protein expression was remarkably increased in nucleoli 24 h after hepatectomy. Although there were variations among samples, NS protein levels appeared to remain elevated at day 3 (Fig. 3B) and reverted to baseline levels at day 7, whereas NS-GFP expression was already downregulated at day 3. Western blotting analysis using an anti-NS antibody consistently showed an increase in endogenous NS protein on day 1 and day 3 after partial hepatectomy (Fig. 3C). The discrepancy between NS-GFP and endogenous NS is possibly due to differences in protein stability stemming from different post-translational modification of these molecules. Interestingly, partial hepatectomy induced a variant form of NS that is reported to be expressed in particular tissues [22,23]. Hepatocytes that had begun to proliferate showed a small increase in the expression of Ki-67, a marker of cell proliferation, at day 1, and further increases in Ki-67 expression were observed at day 3 (Fig. 3A v–viii). These data indicate that NS gene expression is rapidly upregulated before the start of cell division in response to partial hepatectomy.

A DDC diet induces emergence of ductal epithelial cells expressing NS-GFP

DDC treatment inhibits the capacity for hepatocytes to regenerate, while inducing ductal proliferation in mice in what is known as the oval cell response [6]. We found that DDC treatment reduced expression of NS-GFP in hepatocytes (Fig. 4A i, ii) compared to the expression in untreated hepatocytes. We also found that bile duct-like NS-GFP-positive cells emerged in the portal zone following DDC treatment (Fig. 4A iii, iv). Interstitial cells surrounding ductal cells did not express NS-GFP. We confirmed by immunofluorescence that NS-GFP was expressed in $CK19^+$ ductal epithelial cells (Fig. 4B). To investigate the regenerative capacity of NS-GFP-expressing cells in DDC-treated liver, we evaluated NS-GFP intensity in nonparenchymal cells, since oval cells reportedly reside in that population [6]. Flow cytometry analysis showed that most $CD45^-Ter119^-$ nonparenchymal cells were GFP-positive (Fig. 5A), although the intensity of NS-GFP expression in non-parenchymal cells in adult mice appeared lower than that seen in developing liver cells. These NS-GFP-positive cells fell into GFP^{high} and GFP^{low} populations. GFP^{high} cells were relatively rare, but only GFP^{high} cells showed hepatic colony forming ability (Fig. 5C). In contrast, no colonies were generated from GFP^{low} or GFP^{neg} cells. Severe liver injury promoted by a DDC diet increased the proportion of GFP^{high} cells relative to the proportion in untreated mice (Fig. 5B). Because we found that ductal cells express NS-GFP (Figs. 2 and 4), we assumed that the DDC diet increased the number of ductal cells, resulting in an increase in the proportion of GFP^{high} cells. Hepatic colonies were generated only from GFP^{high} cells (Fig. 5D). GFP^{high} cells expressed higher levels of NS mRNA, indicating that GFP expression corresponded with that of endogenous NS, and also expressed several genes reportedly expressed in oval cells [19] (Fig. 5E). These data indicate that hepatic precursor cells induced by severe liver injury express NS.

NS downregulation inhibits proliferation of hepatic precursor cells

Next, to address whether NS is required for regeneration of hepatic precursor cells, we downregulated NS expression in hepatic cell line and primary fetal liver cells in vitro. Previously, we successfully suppressed NS in a germ cell line by infection with a lentivirus carrying NS shRNA [14]. In this system, infected cells were identified by GFP expression driven by the lentivirus vector (GFP^+ cells). For the current study, we infected the mouse hepatocellular carcinoma cell line Hepa1-6 and the mouse embryonic liver cell line BNL C1.2 with lentiviruses carrying NS shRNA (#1 or #2) or a scrambled control shRNA and then stained the cells with an anti-NS antibody. Both shRNAs, but not the scrambled control, efficiently reduced expression of NS protein in the hepatic cell lines (Fig. 6A, data not shown). NS knockdown (GFP^+) cells in the cell lines had dramatically reduced colony-forming capacity (Fig. 6B, data not shown). We also found that NS downregulation significantly decreased the

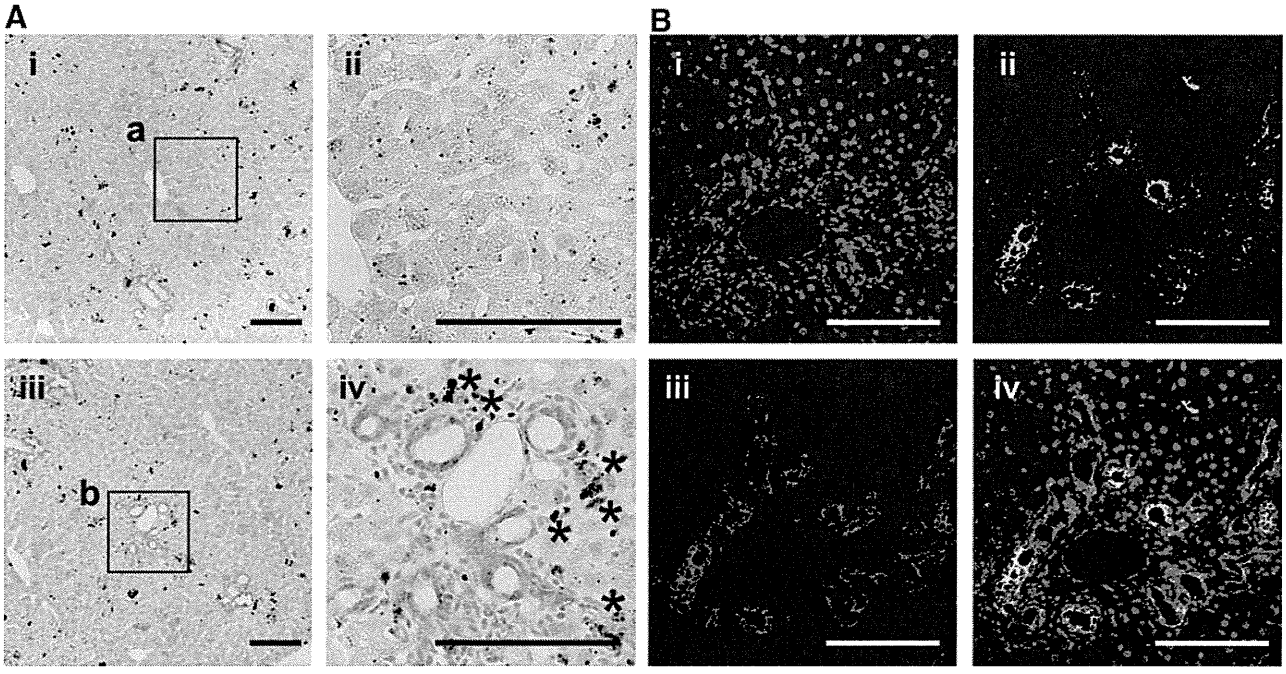

FIG. 4. Duct-like cells express NS-GFP in liver of adult mice fed a 3,5-diethoxycarbonyl-1,4-dihydrocollidine (DDC) diet. **(A, B)** GFP in hepatocytes of adult NS-GFP Tg mice fed a DDC diet. **(A)** Sections were stained with an anti-GFP antibody. **a** and **b** are lower power views of the areas shown at higher power in **(ii)** and **(iv)**, respectively. *Deposition of iron hemes, visible as *brown* clots. **(B)** Sections were stained with anti-GFP (*green*) and anti-CK19 (*red*) antibodies and DAPI (nuclear staining, *blue*). **(i)** DAPI, **(ii)** GFP, **(iii)** CK19, **(iv)** merged. Scale bars, 100 μm.

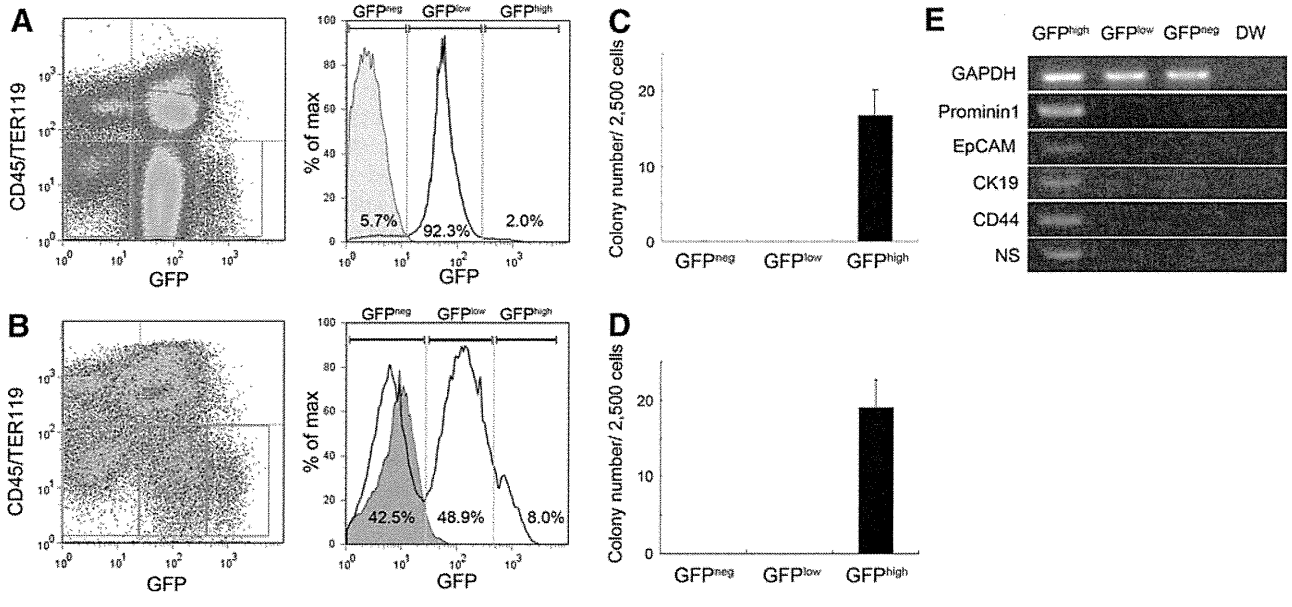

FIG. 5. Increased ratios of NS-GFP^{high} hepatic precursor cells are seen following a DDC diet. **(A, B)** Flow cytometric analyses of GFP expression in nonparenchymal cells of adult NS-GFP Tg mice without **(A)** and with **(B)** a DDC diet. Flow cytometry with CD45/Ter119 and GFP, and a histogram of GFP in CD45$^-$Ter119$^-$ cells are shown in the *left* and *right* panels, respectively. Nonhematopoietic nonparenchymal cells (CD45$^-$Ter119$^-$) were fractionated into 3 distinct subpopulations (GFP^{neg}, GFP^{low}, and GFP^{high} cells). Values in panels are the percentage of the specified subpopulation among CD45$^-$ Ter119$^-$ cells. The data shown are representative of 3 independent experiments. **(C, D)** Hepatic colony formation of subpopulations. Fractionated cells were cultured for 7 days. Data shown are the mean ratio ± SD of colonies derived from mice fed a control **(C)** and DDC **(D)** diet ($n = 3$ each). **(E)** Gene expression in NS-GFP subpopulations. Total RNA was purified from the subpopulations indicated in **(B)**, and mRNA levels of the indicated molecules were evaluated by reverse transcription–polymerase chain reaction. DW, distilled water.

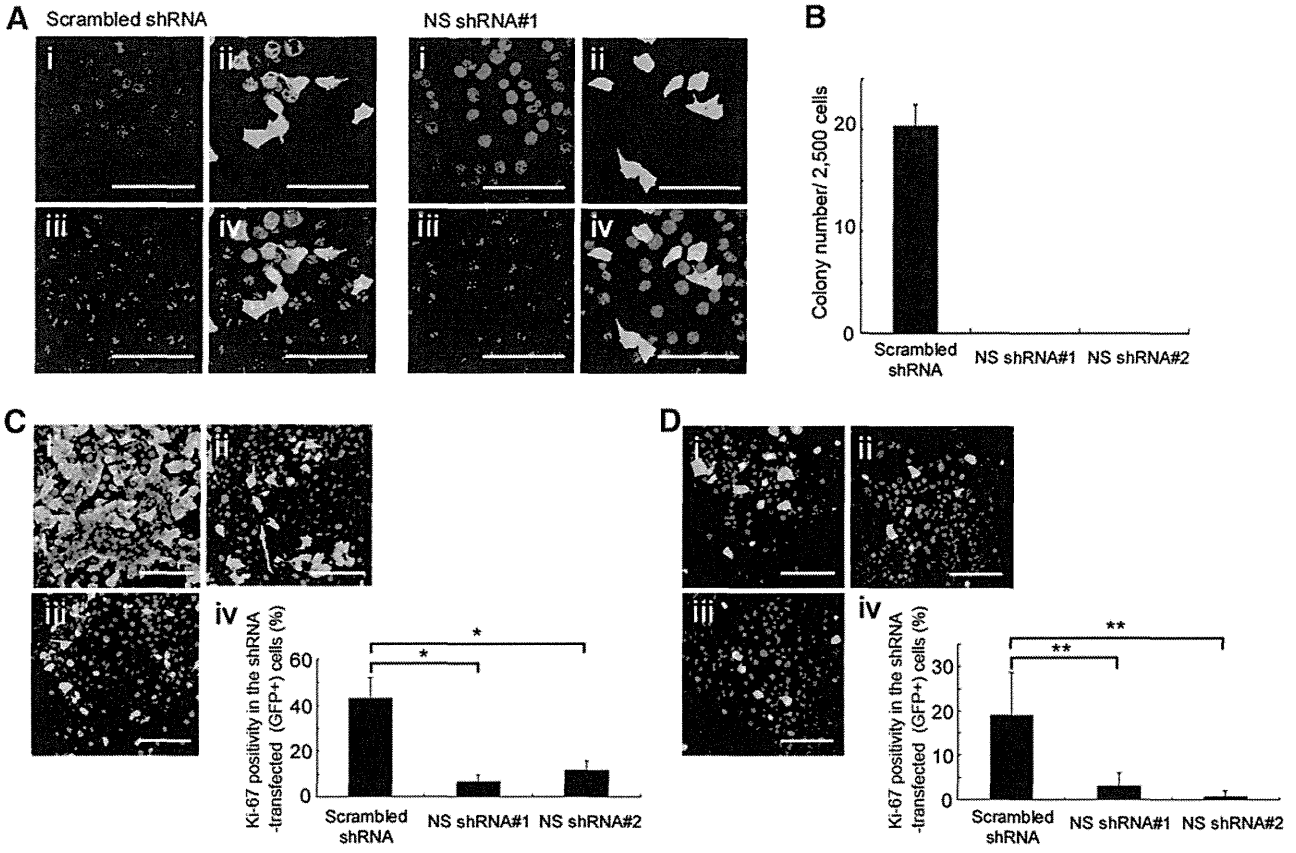

FIG. 6. Inhibition of proliferation of hepatic precursor cells following NS downregulation in vitro. **(A)** NS knockdown in a hepatic cell line. A scrambled shRNA (control, *left panels*) or NS shRNA#1 (*right panels*) was introduced into Hepa1-6 cells (a murine hepatocellular carcinoma cell line) by lentiviral infection, followed by staining with anti-GFP (*green*) and anti-NS (*red*) antibodies and DAPI (*blue*). **(i)** DAPI, **(ii)** GFP, **(iii)** NS, **(iv)** merged. NS protein expression (*red*) was reduced in GFP^+ cells treated with shRNA#1 but not the control shRNA. **(B)** Colony formation of Hepa1-6 cells following NS knockdown. GFP^+ Hepa1-6 cells, indicating those transduced with shRNA, were isolated and cultured for 10 days. Data shown are the mean number ± SD of colonies ($n = 3$). **(C, D)** Proliferation of Hepa1-6 cells **(C)** and Dlk^+ hepatic precursors from fetal liver **(D)** following NS knockdown. Hepa1-6 cells and Dlk^+ fetal liver cells were infected with the shRNA lentivirus, and then cultured for 3 **(C)** or 10 **(D)** days. Cells were stained with an anti-Ki-67 antibody (*red*), anti-GFP antibody (*green*), and DAPI (*blue*). Representative data are shown in **(i)**, **(ii)**, and **(iii)** for the scrambled control, NS shRNA#1, and NS shRNA#2, respectively. Data shown in **(iv)** are the mean ratio ± SD of Ki-67 positivity among cells transfected with the indicated shRNA plasmids (GFP^+ cells) ($n = 3$).*$P < 0.01$, **$P < 0.05$. Scale bars, 100 μm.

proportion of Ki-67-positive cells among transfected (GFP^+) cells in the hepatic cell line (Fig. 6C) and in the hepatic colonies derived from freshly isolated fetal liver precursor cells (Fig. 6D). Thus, NS downregulation inhibits proliferation of hepatic precursor cells.

NS plays an essential role in hepatocyte proliferation in response to liver injury in vivo

The observation that NS is upregulated in hepatocytes after partial hepatectomy suggested that NS is essential for hepatocyte proliferation. To examine the effect of loss NS function in hepatocytes in vivo, we introduced the shRNA plasmids into liver cells by hydrodynamic injection of plasmid DNA via the tail vein [20]. Partial hepatectomy was performed 3 days later and we found that hepatocytes were successfully transfected with shRNA plasmids by detection of GFP expression. Three days after partial hepatectomy, we found that NS knockdown in the hepatocytes significantly suppressed expression of the Ki-67 antigen (Fig. 7), indicating that NS is essential for hepatocyte proliferation in response to liver injury in vivo.

Discussion

In this study, we examined the expression and function of NS in developing and injured liver, and we evaluated the capacity of hepatic NS-expressing cells to form colonies by using an NS-GFP system. As previously reported [19], DDC treatment induced the emergence of ductal cells that express both cholangiocellular and hepatocytic markers, called "oval cells," in periportal regions. Several studies have identified markers of oval cells, including Ep-CAM and CD133 [19,24,25]. NS-GFP was not specific for oval cells, since most hepatocytes and nonparenchymal cells also expressed GFP. Therefore, NS-GFP expression alone cannot be used to purify hepatic stem/precursor cells. However, since a distinct subpopulation of cells expressing high GFP levels (GFP^{high}) showed higher clonogenic potential, combining this system with evaluation of other stem cell markers could enable

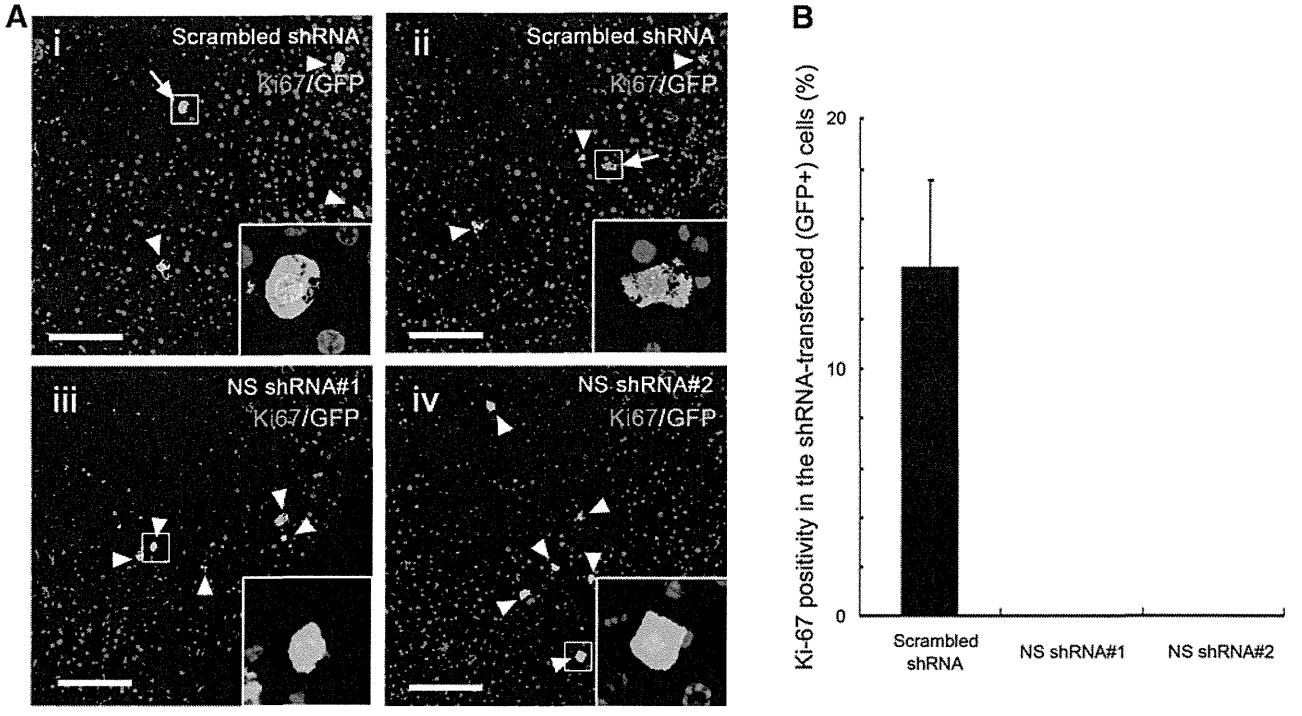

FIG. 7. Inhibition of hepatocyte proliferation following NS downregulation in vivo. NS shRNA plasmids were introduced into liver cells by hydrodynamic injection of the plasmid DNA via the tail vein, followed by partial hepatectomy 3 days after injection. Liver tissue specimens were prepared 3 days later, and sections were stained with an anti-GFP antibody (*green*), anti-Ki-67 antibody (*red*), and DAPI (*blue*). Ki-67 expression was evaluated in more than 60 GFP^+ cells for each sample. **(A)** Representative data for the scrambled control **(i, ii)**, NS shRNA#1 **(iii)**, and NS shRNA#2 **(iv)**. *Arrows*; $GFP^+Ki\text{-}67^+$ cells, *arrowheads*; $GFP^+Ki\text{-}67^-$cells. *Insets* are magnified views of the indicated areas. **(B)** Mean percentage ± SD of Ki-67 positivity in hepatocytes transfected with the indicated shRNA plasmids (GFP^+ cells) ($n=3$). Scale bars, 100 μm.

efficient enrichment of a stem/precursor cell population. In addition, NS may be particularly important for the development of liver, since the expression level of NS-GFP in developing liver cells appeared to be higher than that in adult non-parenchymal cells. NS may therefore play a critical role in expansion of the hepatic stem/precursor cells during liver development.

A previous study demonstrated that NS is required for rRNA processing [9,26], suggesting that NS expression regulates protein synthesis. Enhanced protein synthesis requires activation of ribosomal biogenesis. NS belongs to the class of nucleolar GTPases that includes yeast Nug1, which exports pre-60S ribosomal subunits out of the nucleolus [27]. In *Caenorhabditis elegans*, *nst-1* mutants exhibit reduced rRNA levels, suggesting a critical role of NS in ribosome biogenesis [9]. NS knockdown apparently delays processing of 32S pre-rRNA into 28S rRNA and is accompanied by a substantial decrease in protein synthesis and in the levels of rRNAs and some mRNAs [26]. Because protein synthesis is required for cell growth and proliferation, NS expression in both hepatic precursor cells and hepatocytes may be important for tissue regeneration. On the other hand, protein synthesis appears to be enhanced in resting hepatocytes for reasons unrelated to regeneration. Mature hepatocytes exhibit high levels of protein synthesis to maintain serum protein levels, and protein translation actively occurs even in non-dividing hepatocytes. Thus, NS expression may be controlled by several different signals.

One possible regulator of NS is Myc, which is upregulated by partial hepatectomy [28]. When Myc is overexpressed in mouse hepatocytes in vivo using recombinant adenovirus, hepatocytes enlarge in the absence of significant cell proliferation, an event associated with upregulation of large- and small-subunit ribosomal and nucleolar genes [29]. In addition, a recent study identified the NS gene as a direct transcriptional target of the Myc oncoprotein [22]. Therefore, NS may function to increase cell mass in response to Myc activation following partial hepatectomy. It has also been reported that, constitutive activation of Myc generates hepatocellular carcinoma, whereas Myc inactivation promotes differentiation of tumor cells into hepatocytes and biliary cells, which form bile duct structures [30], suggesting that Myc maintains cells in an undifferentiated status. NS may have a similar function in the case of hepatic malignancy. In addition, Myc may control post-translational regulation of NS protein. A recent study revealed that NS is a target of reactive oxygen species (ROS) [31]. In transformed hematopoietic cells, Myc activation leads to high ROS levels, resulting in impaired NS protein degradation. Therefore, Myc activation may stabilize NS protein in regenerating liver. Because GFP would not be stabilized in the same way as the NS protein, these findings suggest that NS protein levels may not be precisely correlated with NS-GFP levels. Nonetheless, both NS protein levels and NS-GFP expression are consistently upregulated by partial hepatectomy. These findings suggest that overall NS expression is likely regulated by both transcriptional and protein stability.

In conclusion, we have demonstrated that NS is essential for proliferation of both hepatic precursor cells and

hepatocytes. Understanding the mechanisms regulating NS expression and function may contribute to development of methodologies useful for enhancing liver regeneration in pathological states.

Acknowledgments

We thank Drs. Akihide Kamiya, Hiromitsu Nakauchi, Tetsuhiro Chiba, Atsushi Iwama, and Atsushi Miyajima for providing information and technical advice for establishing assay systems for hepatic colony formation and isolation of liver cells and Dr. Kenichi Harada for insightful suggestions for histological analyses. A.H. was supported by a Grant-in-Aid for Scientific Research on Innovative Areas and the Project for Development of Innovative Research on Cancer Therapeutics (P-DIRECT) from the Ministry of Education, Culture, Sports, Science and Technology, Japan, and by a grant from the Japan Science and Technology Agency (JST), CREST.

Author Disclosure Statement

No competing financial interests exist.

References

1. Michalopoulos GK and MC DeFrances. (1997). Liver regeneration. Science 276:60–66.
2. Michalopoulos GK. (2010). Liver regeneration after partial hepatectomy: critical analysis of mechanistic dilemmas. Am J Pathol 176:2–13.
3. Tanaka M, T Itoh, N Tanimizu and A Miyajima. (2011). Liver stem/progenitor cells: their characteristics and regulatory mechanisms. J Biochem 149:231–239.
4. Oertel M and DA Shafritz. (2008). Stem cells, cell transplantation and liver repopulation. Biochim Biophys Acta 1782:61–74.
5. Farber E. (1956). Similarities in the sequence of early histological changes induced in the liver of the rat by ethionine, 2-acetylamino-fluorene, and 3'-methyl-4-dimethylaminoazobenzene. Cancer Res 16:142–148.
6. Preisegger KH, VM Factor, A Fuchsbichler, C Stumptner, H Denk and SS Thorgeirsson. (1999). Atypical ductular proliferation and its inhibition by transforming growth factor beta1 in the 3,5-diethoxycarbonyl-1,4-dihydrocollidine mouse model for chronic alcoholic liver disease. Lab Invest 79:103–109.
7. Tsai RY and RD McKay. (2002). A nucleolar mechanism controlling cell proliferation in stem cells and cancer cells. Genes Dev 16:2991–3003.
8. Nomura J, M Maruyama, M Katano, H Kato, J Zhang, S Masui, Y Mizuno, Y Okazaki, M Nishimoto and A Okuda. (2009). Differential requirement for nucleostemin in embryonic stem cell and neural stem cell viability. Stem Cells 27:1066–1076.
9. Kudron MM and V Reinke. (2008). *C. elegans* nucleostemin is required for larval growth and germline stem cell division. PLoS Genet 4:e1000181.
10. Maki N, K Takechi, S Sano, H Tarui, Y Sasai and K Agata. (2007). Rapid accumulation of nucleostemin in nucleolus during newt regeneration. Dev Dyn 236:941–950.
11. Beekman C, M Nichane, S De Clercq, M Maetens, T Floss, W Wurst, E Bellefroid and JC Marine. (2006). Evolutionarily conserved role of nucleostemin: controlling proliferation of stem/progenitor cells during early vertebrate development. Mol Cell Biol 26:9291–9301.
12. Han C, X Zhang, W Xu, W Wang, H Qian and Y Chen. (2005). Cloning of the nucleostemin gene and its function in transforming human embryonic bone marrow mesenchymal stem cells into F6 tumor cells. Int J Mol Med 16: 205–213.
13. Hirai H, L Romanova, S Kellner, M Verma, S Rayner, A Asakura and N Kikyo. (2010). Post-mitotic role of nucleostemin as a promoter of skeletal muscle cell differentiation. Biochem Biophys Res Commun 391:299–304.
14. Ohmura M, K Naka, T Hoshii, T Muraguchi, H Shugo, A Tamase, N Uema, T Ooshio, F Arai, et al. (2008). Identification of stem cells during prepubertal spermatogenesis via monitoring of nucleostemin promoter activity. Stem Cells 26:3237–3246.
15. Tamase A, T Muraguchi, K Naka, S Tanaka, M Kinoshita, T Hoshii, M Ohmura, H Shugo, T Ooshio, et al. (2009). Identification of tumor-initiating cells in a highly aggressive brain tumor using promoter activity of nucleostemin. Proc Natl Acad Sci U S A 106:17163–17168.
16. Lin T, L Meng, Y Li and RY Tsai. (2010). Tumor-initiating function of nucleostemin-enriched mammary tumor cells. Cancer Res 70:9444–9452.
17. Okamoto N, M Yasukawa, C Nguyen, V Kasim, Y Maida, R Possemato, T Shibata, KL Ligon, K Fukami, WC Hahn and K Masutomi. (2011). Telomerase and retrotransposons: reverse transcriptases that shaped genomes special feature sackler colloquium: maintenance of tumor initiating cells of defined genetic composition by nucleostemin. Proc Natl Acad Sci U S A 108:20388–20393.
18. Kamiya A, T Kinoshita, Y Ito, T Matsui, Y Morikawa, E Senba, K Nakashima, T Taga, K Yoshida, T Kishimoto and A Miyajima. (1999). Fetal liver development requires a paracrine action of oncostatin M through the gp130 signal transducer. EMBO J 18:2127–2136.
19. Okabe M, Y Tsukahara, M Tanaka, K Suzuki, S Saito, Y Kamiya, T Tsujimura, K Nakamura and A Miyajima. (2009). Potential hepatic stem cells reside in EpCAM+ cells of normal and injured mouse liver. Development 136: 1951–1960.
20. Zhang G, V Budker and JA Wolff. (1999). High levels of foreign gene expression in hepatocytes after tail vein injections of naked plasmid DNA. Hum Gene Ther 10:1735–1737.
21. Tanimizu N, M Nishikawa, H Saito, T Tsujimura and A Miyajima. (2003). Isolation of hepatoblasts based on the expression of Dlk/Pref-1. J Cell Sci 116:1775–1786.
22. Zwolinska AK, A Heagle Whiting, C Beekman, JM Sedivy and JC Marine. (2011). Suppression of Myc oncogenic activity by nucleostemin haploinsufficiency. Oncogene 2011 [Epub ahead of print]; DOI: 10.1038/onc.2011.507.
23. Malakootian M, SJ Mowla, H Saberi, MH Asadi, Y Atlasi and AM Shafaroudi. (2010). Differential expression of nucleostemin, a stem cell marker, and its variants in different types of brain tumors. Mol Carcinog 49:818–825.
24. Suzuki A, S Sekiya, M Onishi, N Oshima, H Kiyonari, H Nakauchi and H Taniguchi. (2008). Flow cytometric isolation and clonal identification of self-renewing bipotent hepatic progenitor cells in adult mouse liver. Hepatology 48:1964–1978.
25. Kamiya A, S Kakinuma, Y Yamazaki and H Nakauchi. (2009). Enrichment and clonal culture of progenitor cells during mouse postnatal liver development in mice. Gastroenterology 137:1114–1126.

26. Romanova L, A Grand, L Zhang, S Rayner, N Katoku-Kikyo, S Kellner and N Kikyo. (2009). Critical role of nucleostemin in pre-rRNA processing. J Biol Chem 284:4968–4977.
27. Bassler J, P Grandi, O Gadal, T Lessmann, E Petfalski, D Tollervey, J Lechner and E Hurt. (2001). Identification of a 60S preribosomal particle that is closely linked to nuclear export. Mol Cell 8:517–529.
28. Morello D, MJ Fitzgerald, C Babinet and N Fausto. (1990). c-myc, c-fos, and c-jun regulation in the regenerating livers of normal and H-2K/c-myc transgenic mice. Mol Cell Biol 10:3185–3193.
29. Kim S, Q Li, CV Dang and LA Lee. (2000). Induction of ribosomal genes and hepatocyte hypertrophy by adenovirus-mediated expression of c-Myc *in vivo*. Proc Natl Acad Sci U S A 97:11198–11202.
30. Shachaf CM, AM Kopelman, C Arvanitis, A Karlsson, S Beer, S Mandl, MH Bachmann, AD Borowsky, B Ruebner, et al. (2004). MYC inactivation uncovers pluripotent differentiation and tumour dormancy in hepatocellular cancer. Nature 431:1112–1117.
31. Huang M, P Whang, JV Chodaparambil, DA Pollyea, B Kusler, L Xu, DW Felsher and BS Mitchell. (2011). Reactive oxygen species regulate nucleostemin oligomerization and protein degradation. J Biol Chem 286:11035–11046.

Address correspondence to:
Dr. Atsushi Hirao
Division of Molecular Genetics
Cancer Research Institute
Kanazawa University
Kakuma-machi
Kanazawa, Ishikawa 920-1192
Japan

E-mail: ahirao@staff.kanazawa-u.ac.jp

Received for publication December 25, 2011
Accepted after revision May 10, 2012
Prepublished on Liebert Instant Online July 9, 2012

HEPATOLOGY
Official Journal of the American Association for the Study of Liver Diseases

Severe Necroinflammatory Reaction Caused by Natural Killer Cell-Mediated Fas/Fas Ligand Interaction and Dendritic Cells in Human Hepatocyte Chimeric Mouse

Akihito Okazaki,[1,2] Nobuhiko Hiraga,[1,2] Michio Imamura,[1,2] C. Nelson Hayes,[1,2,3] Masataka Tsuge,[1,2] Shoichi Takahashi,[1,2] Hiroshi Aikata,[1,2] Hiromi Abe,[1,2,3] Daiki Miki,[1,2,3] Hidenori Ochi,[1,2,3] Chise Tateno,[2,4] Katsutoshi Yoshizato,[2,4] Hideki Ohdan,[2,5] and Kazuaki Chayama[1,2,3]

The necroinflammatory reaction plays a central role in hepatitis B virus (HBV) elimination. Cluster of differentiation (CD)8-positive cytotoxic T lymphocytes (CTLs) are thought to be a main player in the elimination of infected cells, and a recent report suggests that natural killer (NK) cells also play an important role. Here, we demonstrate the elimination of HBV-infected hepatocytes by NK cells and dendritic cells (DCs) using urokinase-type plasminogen activator/severe combined immunodeficiency mice, in which the livers were highly repopulated with human hepatocytes. After establishing HBV infection, we injected human peripheral blood mononuclear cells (PBMCs) into the mice and analyzed liver pathology and infiltrating human immune cells with flow cytometry. Severe hepatocyte degeneration was observed only in HBV-infected mice transplanted with human PBMCs. We provide the first direct evidence that massive liver cell death can be caused by Fas/Fas ligand (FasL) interaction provided by NK cells activated by DCs. Treatment of mice with anti-Fas antibody completely prevented severe hepatocyte degeneration. Furthermore, severe hepatocyte death can be prevented by depletion of DCs, whereas depletion of CD8-positive CTLs did not disturb the development of massive liver cell apoptosis. *Conclusion:* Our findings provide the first direct evidence that DC-activated NK cells induce massive HBV-infected hepatocyte degeneration through the Fas/FasL system and may indicate new therapeutic implications for acute severe/fulminant hepatitis B. (HEPATOLOGY 2012;56:555-566)

Between 4% and 32% of fulminant hepatitis cases, characterized by acute massive hepatocyte degeneration and subsequent development of hepatic encephalopathy and liver failure, are caused by acute hepatitis B virus (HBV) infection.[1] Host[2] and viral factors[3] may influence the development of fulminant hepatitis, but these factors have not been fully elucidated.

Innate and adaptive immunity both play a role in the elimination of viral infections. In the innate immune response, cytoplasmic and membrane-bound receptors recognize viruses and induce interferon (IFN)-β production, which, in turn, up-regulates IFN-α and induces an antiviral state in surrounding cells.[4] In the adaptive immune response, viruses are recognized by dendritic cells (DCs), which activate cluster of differentiation (CD)8-positive T cells to reduce viral replication through cytolytic[5] and noncytolytic mechanisms.[6] The role of immune cells, especially HBV-specific cytotoxic T lymphocytes (CTLs), is crucial in the

Abbreviations: APC, allophycocyanin; asialo GM1, ganglio-N-tetraosylceramide; CD, cluster of differentiation; CHB, chronic hepatitis B; CTLs, cytotoxic T lymphocytes; DC, dendritic cell; FasL, Fas ligand; FHB, fulminant hepatitis B; HBcAg, hepatitis B core antigen; HBsAg, hepatitis B surface antigen; HBV, hepatitis B virus; HLA, human leukocyte antigen; HSA, human serum albumin; IFN, interferon; IP, intraperitoneally; ISG, interferon-stimulated gene; mAb, monoclonal antibody; mDC, myeloid DC; mRNA, messenger RNA; NK, natural killer; PBMCs, peripheral blood mononuclear cells; PCR, polymerase chain reaction; pDC, plasmacytoid DC; SCID, severe combined immunodeficiency; TUNEL, terminal deoxynucleotidyl transferase dUTP nick end labeling; uPA, urokinase-type plasminogen activator.

From the [1]Department of Medicine and Molecular Science, Division of Frontier Medical Science, Programs for Biomedical Research, Graduate School of Biomedical Sciences, Hiroshima University, Hiroshima, Japan; [2]Liver Research Project Center, Hiroshima University, Hiroshima, Japan; [3]Laboratory for Digestive Diseases, Center for Genomic Medicine, RIKEN, Hiroshima, Japan; [4]PhoenixBio Co., Ltd., Higashi-Hiroshima, Japan; and [5]Department of Surgery, Division of Frontier Medical Science, Programs for Biomedical Research, Graduate School of Biomedical Science, Hiroshima University, Hiroshima, Japan.

Received August 16, 2011; accepted February 4, 2012.

This study was supported, in part, by a Grant-in-Aid for Scientific Research from the Japanese Ministry of Labor, Health, and Welfare.

development of fulminant hepatitis.[7,8] CTLs can kill target cells using two distinct lytic pathways: the degranulation pathway, in which perforin is used to puncture the membranes of infected cells, and the Fas-based pathway, in which the interaction between Fas ligand (FasL) expressed on cytolytic lymphocytes and Fas on target cells triggers apoptosis and target cell death.[9] However, the role of innate immune cells, especially natural killer (NK) cells, in fulminant hepatitis remains obscure. NK cells have recently been reported to contribute to the pathogenesis of human hepatitis and animal models of liver injury.[10,11] Replication of HBV is host cell dependent, and the study of cellular immune response in hepatitis B has long been hampered by the lack of a small animal model that supports the replication of HBV and elimination of infected cells by immune response. Before the advent of human hepatocyte chimeric mice,[12,13] only chimpanzees had been used as a model for HBV infection and inflammation, although fulminant hepatitis B (FHB) had never been reported, and severe liver inflammation is rare in chimpanzees.[14] We previously established an HBV-infection animal model using chimeric mice, in which the livers were extensively repopulated with human hepatocytes.[15-17] In this study, we attempted to establish an animal model of HBV-infected human hepatocytes with human immunity by transplanting human peripheral mononuclear cells (PBMCs) to HBV-infected human hepatocyte chimeric mice.

Materials and Methods

Generation of Human Hepatocyte Chimeric Mice. Generation of the urokinase-type plasminogen activator (uPA)$^{+/+}$/severe combined immunodeficiency (SCID)$^{+/+}$ mice and transplantation of human hepatocytes with human leukocyte antigen (HLA)-A0201 were performed as described previously.[15,16] All mice were transplanted with frozen human hepatocytes obtained from the same donor. Infection, extraction of serum samples, and euthanasia were performed under ether anesthesia. Concentration of human albumin, which is correlated with the repopulation index,[15] was measured in mice as described previously.[16] All animal protocols described in this study were performed in accord with the *Guide for the Care and Use of Laboratory Animals* and the local committee for animal experiments, and the experimental protocol was approved by the Ethics Review Committee for Animal Experimentation of the Graduate School of Biomedical Sciences at Hiroshima University (Hiroshima, Japan).

Human Serum Samples. Human serum samples, containing high titers of genotype C HBV DNA (5.3×10^6 copies/mL), were obtained from patients with chronic hepatitis who provided written informed consent. Individual serum samples were divided into aliquots and stored in liquid nitrogen. Six weeks after hepatocyte transplantation, chimeric mice were injected intravenously with 50 μL of HBV-positive human serum.

Analysis of HBV. DNA was extracted using SMITEST (Genome Science Laboratories, Tokyo, Japan) and dissolved in 20 μL of H_2O. HBV DNA was measured by real-time polymerase chain reaction (PCR) using a light cycler (Roche, Mannheim, Germany). Primers used for amplification were 5′-TTTGGGCATGGACATTGAC-3′ and 5′-GGTGA ACAATGTTCCGGAGAC-3′. Amplification conditions included initial denaturation at 95°C for 10 minutes, followed by 45 cycles of denaturation at 95°C for 15 seconds, annealing at 58°C for 5 seconds, and extension at 72°C for 6 seconds. The lower detection limit of this assay was 300 copies.

Preparation of Human Blood Mononuclear Cells and Transplantation of Human PBMCs Into Human Hepatocyte Chimeric Mice. PBMCs were isolated from healthy blood donors with HLA-A0201 and successfully vaccinated with recombinant yeast-derived hepatitis B surface antigen (HBsAg) vaccine (Bimmugen; Chemo-Sero Therapeutic Institute, Kumamoto, Japan) using Ficoll-Hypaque density gradient centrifugation. Neither monocytes nor macrophages were observed in the isolated PBMCs (Supporting Fig. 1). PBMCs isolated from 3 healthy, unvaccinated blood donors were also transplanted. Eight weeks after HBV inoculation, human PBMCs were transplanted into human hepatocyte chimeric mice. To deplete mouse NK cells and prevent the elimination of human PBMCs from human hepatocyte

Address reprint requests to: Kazuaki Chayama, M.D., Ph.D., Department of Medical and Molecular Science, Division of Frontier Medical Science, Programs for Biomedical Research, Graduate School of Biomedical Science, Hiroshima University, 1-2-3 Kasumi, Minami-ku, Hiroshima 734-8551, Japan. E-mail: chayama@hiroshima-u.ac.jp; fax: +81-82-255-6220.

View this article online at wileyonlinelibrary.com.
DOI 10.1002/hep.25651
Potential conflict of interest: The authors have no conflicts to disclose.
Additional Supporting Information may be found in the online version of this article.

chimeric mice, 200 μL of phosphate-buffered saline, containing 120 μL of anti–ganglio-N-tetraosylceramide (asialo GM1) antibody (Wako, Osaka, Japan), were administered intraperitoneally (IP) 1 day before (day 0; Fig. 1) the initial IP transplantation (day 1) of human PBMC. Then, 10 μL/g of liposome-encapsulated clodronate (Sigma-Aldrich, St. Louis, MO) were also administered 4 days before PBMC transplantation (day −2) to deplete mouse macrophages and DC cells. The second PBMC administration (4×10^7 cells/mouse) was performed 2 days after the initial administration (day 3).

To assess the effect of the depletion of human DC, NK, or CD8-positive CTL cells from administered PBMCs on hepatitis formation, the BD IMag separation system (BD Biosciences, Franklin Lakes, NJ) was used. Alternatively, mice were treated with an IP administration of clodronate, as described above, 1 day before PBMC transplantation.

To analyze the effect of inhibition of the Fas/FasL system, IFN-γ, IFN-α, antihuman FasL monoclonal antibody (mAb) (1.5 mg/mouse; R&D Systems, Minneapolis, MN), antihuman IFN-γ mAb (1.5 mg/mouse; R&D Systems), and antihuman IFN-α mAb (1.5 mg/mouse; PBL Biomedical Laboratories, Piscataway, NJ) were injected 1 day before transplantation of human PBMCs.

Flow Cytometry. Reconstructed human PBMC proliferation in mice was determined by flow cytometry with the following mAbs used for PBMC surface staining: allophycocyanin (APC)-H7 antihuman CD3 (clone SK7); APC-conjugated anti-CD4 (clone SK); BD Horizon V450 antihuman CD8 (clone RPA-T8); APC-conjugated antihuman CD11c (clone B-ly6); HU HRZN V500 MAB-conjugated antihuman CD45 (clone H130); Alexa Fluor 488–conjugated antihuman CD56 (clone B159); PerCP-Cy5.5 antihuman CD123 (clone 7G3); fluorescein isothiocyanate–conjugated Lineage cocktail 1 (Lin-1) (anti-CD3, CD14, CD16, CD19, CD20, and CD56); APC-H7 antihuman HLA-DR (clone L243); phycoerythrin (PE)-conjugated antihuman FasL (clone NOK-1); and biotin-conjugated antimouse H-$2D^b$ (clone KH95). The biotinylated mAbs were visualized using PE-Cy7-streptavidin. Each of the above mAbs were purchased from BD Biosciences. PE-conjugated HBV core-derived immunodominant CTL epitope (HBcAg93)[18] (Medical & Biological Laboratories Co., Ltd., Nagoya, Japan). Dead cells identified by light scatter and propidium iodide staining were excluded from the analysis. Flow cytometry was performed using a FACSAria II flow cytometer (BD Biosciences), and results were analyzed with FlowJo software (Tree Star, Inc., Ashland, OR).

DCs can be classified into two main subsets: plasmacytoid DCs (pDCs) and myeloid DCs (mDCs).[19,20] pDCs were defined as $CD45^+$Lin-1^-HLA-DR^+CD123^+ cells, whereas mDCs were defined as $CD45^+$ Lin-1^-HLA-DR^+CD11c^+ cells.

Histochemical Analysis of Mouse Liver and Terminal Deoxynucleotidyl Transferase dUTP Nick End Labeling Assay. Histochemical analysis and immunohistochemical staining using an antibody against human serum albumin (HSA; Bethyl Laboratories, Inc., Montgomery, TX), an antibody against hepatitis B core antigen (HBcAg) (Dako Diagnostika, Hamburg, Germany) and antibody against Fas (BD Biosciences, Tokyo, Japan) were performed as described previously.[16] Immunoreactive materials were visualized using a streptavidin-biotin staining kit (Histofine SAB-PO kit; Nichirei, Tokyo, Japan) and diainobenzidine. For the terminal deoxynucleotidyl transferase dUTP nick end labeling (TUNEL) assay in sliced tissues, we used an *in situ* cell death detection kit (POD; Roche Diagnostics Japan, Tokyo, Japan).

Dissection of Mouse Livers and Isolation of RNA and Measurement of Messenger RNAs of Fas by Reverse-Transcription PCR. Mice were sacrificed by anesthesia with diethyl ether, and livers were excised, dissected into small sections, and then snap-frozen in liquid nitrogen. Total RNA was extracted from cell lines using the RNeasy Mini Kit (Qiagen, Valencia, CA). One microgram of each RNA sample was reverse transcribed with ReverseTra Ace (Toyobo Co., Tokyo, Japan) and Random Primer (Takara Bio Inc., Kyoto, Japan). We analyzed the messenger RNA (mRNA) levels of Fas by reverse-transcription PCR, as previously reported, using Fas forward primer 5′-GGGCATCTGGACCCTCCTA-3′ and Fas reverse primer 5′- GGCATTAACACTTTTGGACGATAA-3′.

Statistical Analysis. mRNA expression levels of Fas and interferon-stimulated genes (ISGs) were compared using Mann-Whitney's U test and unpaired *t* tests. A *P* value less than 0.05 was considered statistically significant.

Results

Establishment of an Animal Model of Fulminant Hepatitis Using HBV-Infected Human Hepatocyte Chimeric Mice and Human PBMC Transplantation. Administration of 2×10^7 PBMCs twice after suppression of mice NK cells by anti–asialo GM1 antibody[21] and macrophages and DCs by liposome-encapsulated clodronate[22] before transplantation

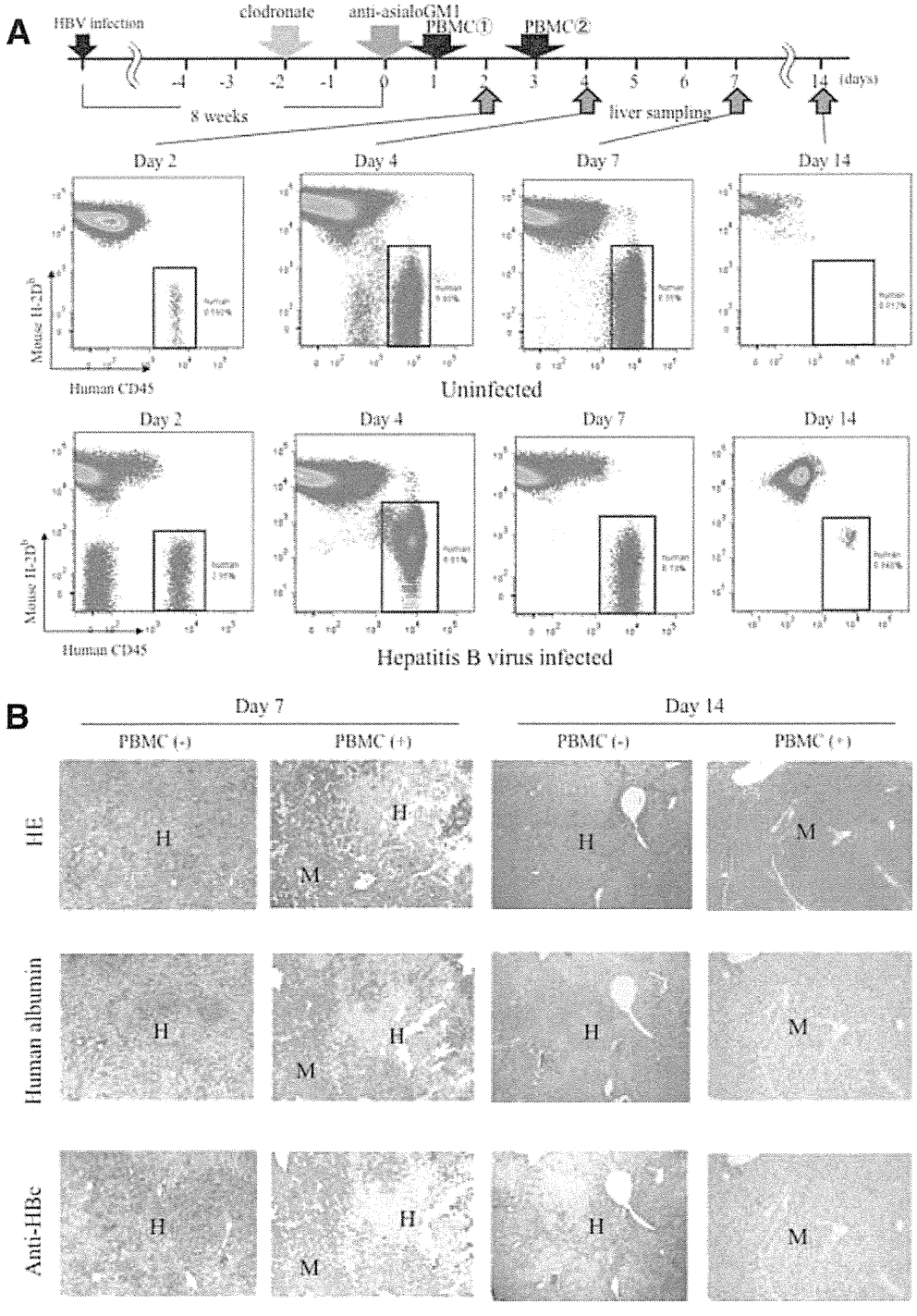

Fig. 1. Establishment of human PBMC chimerism in human hepatocyte chimeric mice. (A) Experimental protocol to establish chimerism and liver sampling is shown at the top of the figure (see Materials and Methods). Scheduling of administration of HBV-positive serum, clodronate, and anti-asialo GM1 antibody and liver sampling by scarification are shown by arrows. Liver mononuclear cells isolated from uninfected (upper panel) and HBV-infected (lower panel) human hepatocyte chimeric mice transplanted with human PBMCs were separated with antibodies for human CD45 and mouse H-2D^b and were analyzed by flow cytometry. Percentage of human mononuclear cells is shown in each panel. Representative figures of two experiments with similar results are shown. (B) Histological analysis of livers of HBV-infected mice. Liver samples obtained from mice with or without human PBMCs at weeks 9 (day 7) and 10 (day 14) were stained with hematoxylin and eosin staining (HE), anti-human albumin antibody, or anti-hepatitis B core antibody. Regions are shown as human (H) and mouse (M) hepatocytes, respectively (original magnification, 40×). (C) Time course of human albumin concentration (upper panel) and HBV DNA titer (lower panel) in mouse serum. Time course of 4 HBV-infected mice transplanted with human PBMCs, 3 HBV-infected mice without human PBMC transplantation, and 4 uninfected mice transplanted with human PBMC are shown. (D) Time course of human albumin concentration (upper panel) and HBV DNA titer (lower panel) in mice. Mice with or without HBV-infection were transplanted with PBMCs obtained from 3 healthy donors who were not vaccinated against hepatitis B.

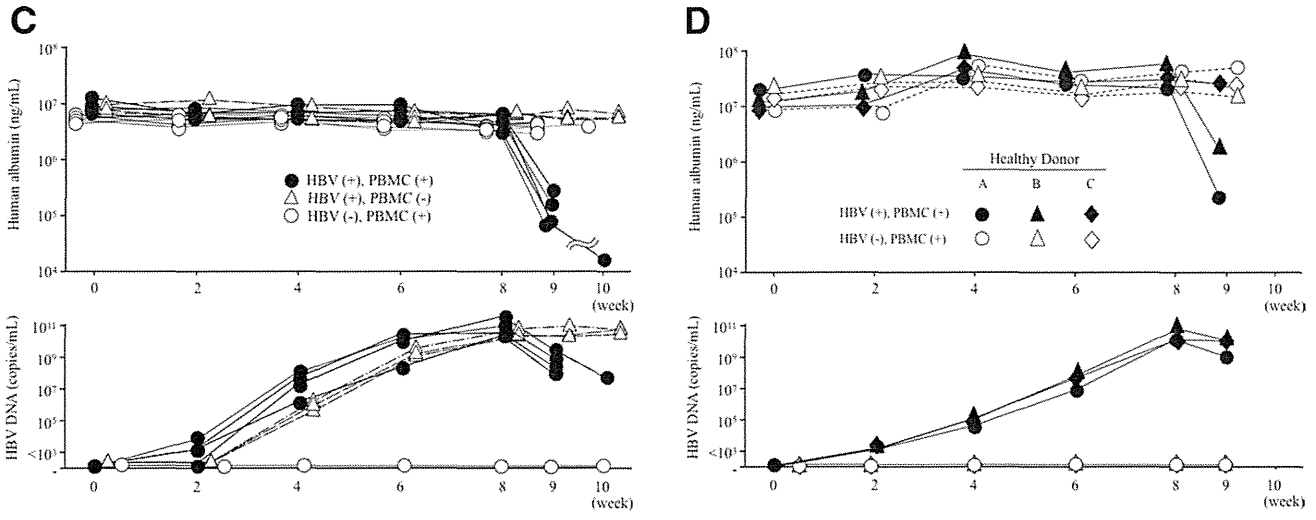

Fig. 1.

enabled us to establish a human PBMC chimerism in uPA-SCID mice. We observed an up to 7% human mononuclear cell chimerism among the liver-resident mononuclear cells of uninfected and HBV-infected mice 2-14 days after the initial injection of PBMC (Fig. 1A; Table 1). Chimerism was most prominent 4 days after initial PBMC administration and almost undetectable by day 14 (Fig. 1A). Histological examination of chimeric mice livers showed extensive human liver cell death, comparable to the massive liver cell death observed in fulminant hepatitis, only in HBV-infected and PBMC-treated mice liver (Fig. 1B). Human hepatocytes were almost completely eliminated and replaced by human albumin-negative mouse hepatocytes at days 7 and 14. Consistent with these histological changes, we observed a rapid decline of HSA levels and HBV DNA only in HBV-infected and PBMC-treated mice (Fig. 1C). The decline of mice HSA levels and HBV DNA was also observed in 2 of 3 HBV-infected mice transplanted with PBMCs isolated from healthy blood donors without HBsAg vaccination (Fig. 1D and Supporting Fig. 2).

Analysis of Liver-Infiltrating Human Lymphocytes Necessary to Establish Massive Hepatocyte Degeneration. We then analyzed liver-infiltrating cells with flow cytometry. Unexpectedly, we did not detect CD8-positive and tetramer-positive CTLs, as reported previously (Fig. 2A). Instead, we observed substantial numbers of CD3-negative and CD56-positive NK cells (Fig. 2B) and small numbers of pDCs and mDCs (Fig. 2C). The majority of NK cells of HBV-infected mice were FasL positive (Fig. 2D). In contrast, such FasL-positive NK cells were not detected in uninfected

Table 1. Analysis of Liver-Infiltrating Cells by Flow Cytometry

	HBV Infected				Uninfected			
Day	No.	Chimerism (%)	Human NK (%)	Fas (+) NK (%)	No.	Chimerism (%)	Human NK (%)	FasL (+) NK (%)
2	1	1.77	2.51	0	1	0.59	12.8	0
	2	2.35	3.02	0.143	2	0.774	58.8	1.1
4	3	6.81	30.7	80.1	3	5.95	42.7	0.678
	4	1.08	68.7	94.7	4	7.11	4.98	0.027
	5	6.60	23.2	58.7	5	5.02	23.1	0.314
7	6	6.73	13.2	0.383	6	6.55	42.1	0.103
	7	5.70	12.5	2.01	7	1.24	13.6	0.025
	8	1.46	3.83	0	8	2.04	1.49	4.03
14	9	0.34	ND	ND	9	0.012	ND	ND
	10	NA*	NA	NA	10	0.013	ND	ND
DCs depleted day 4	11	4.77	5	2.14	11	3.32	4.21	0.465
(by clodronate)	12	1.27	39.5	2.3	12	12.9	9.06	0
DCs depleted day 7	13	2.42	24.8	2.19	13	6.31	54.1	0.131
(by clodronate)	14	1.41	10.6	0.103	14	4.69	1.68	0.12

Abbreviations: NA, not analyzed; ND, not detectable.
*Mouse died just before liver analysis.

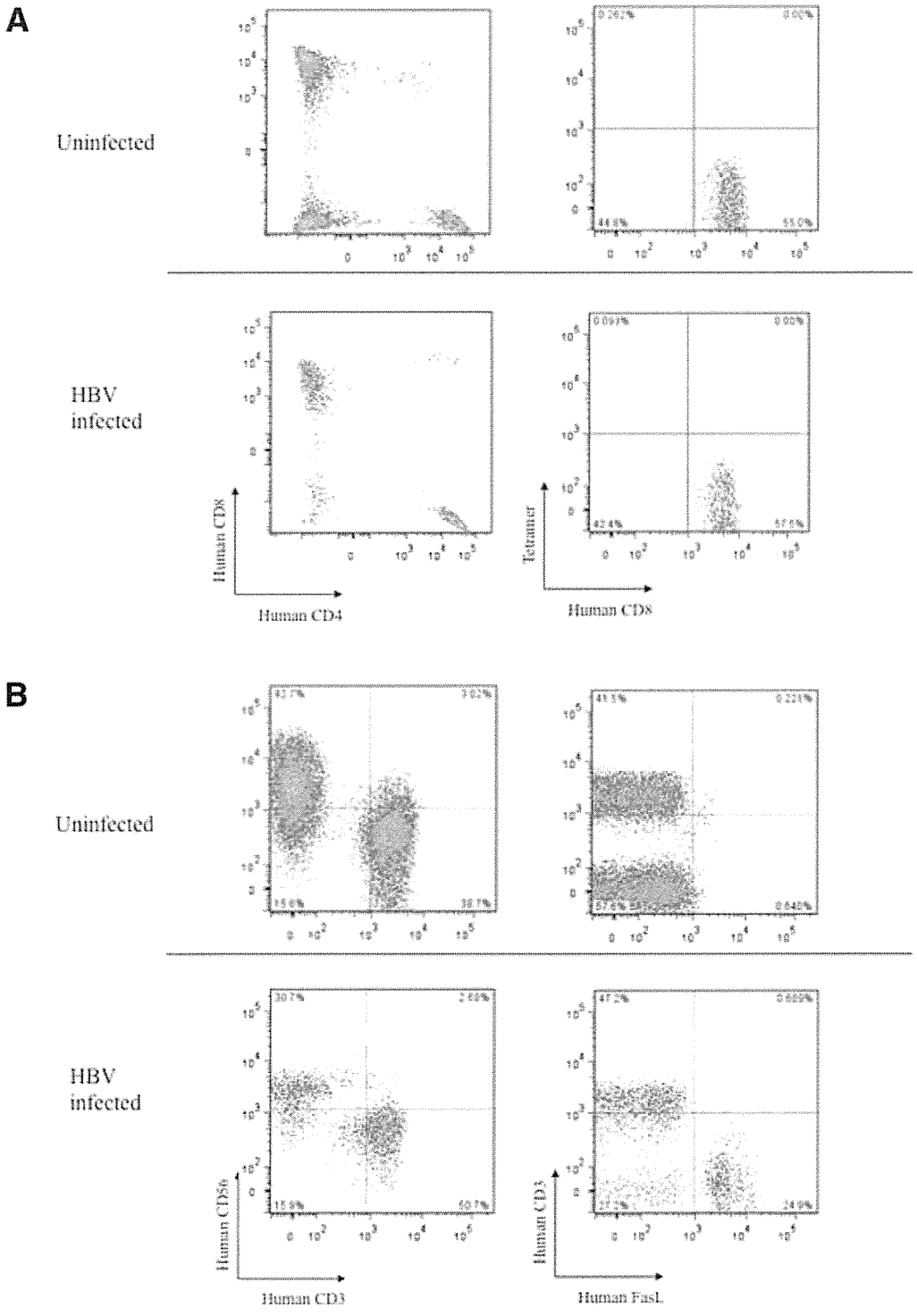

Fig. 2. Analysis of mononuclear cells isolated from day 4 chimeric mouse livers. After defining human PBMCs as mouse H-2Db-human CD45^{+} cells, we further analyzed the phenotypes of these cells. (A-C) Liver mononuclear cells of uninfected (upper panel) and HBV-infected (lower panel) mice transplanted with human PBMCs were separated with anti-human CD4 and CD8 antibody or anti-human CD8 and HLA-A2 HBcAg tetramer (A), anti-human CD3and CD56 or human CD3 and FasL (B), and anti-human HLA-DR and CD123 and HLA-DR and CD11c (C). (D) Frequency of FasL-positive cells in NK cells were analyzed in uninfected and HBV-infected mice. All figures are representative of two experiments with similar results.

mice livers (Table 1; Fig. 2D), suggesting that these NK cells were activated in HBV-infected mice. These activated NK cells and DCs were detectable in mice livers only 4 days after the initial PBMC injection, but were undetectable after 2 and 7 days (Supporting Figs. 3 and 4, respectively).